Chapter 8

Brownian motion, weather and climate

The daily observed maximum and minimum temperatures is often compared to the "normal" temperatures based upon the 30-year average. Climate averages provide a context for something like "this winter will be wetter (or drier, or colder, or warmer, etc.) than normal. It has been said "Climate is what you expect. Weather is what you get."

What is the difference between weather and climate? This can be also answered by an example/a methaphor in the football league. Predicting the outcome of the next game is difficult (weather), but predicting who will end up as German champion is unfortunately relatively easy (climate). In this section, I will give a general approach to the mean and fluctuations in the climate system. Indeed, the Brownian motion approach is a helpful analogue for weather and climate.

Brownian motion

The Roman Lucretius's scientific poem On the Nature of Things (ca. 60 BC) has a remarkable description of Brownian motion of dust particles[1]. Jan Ingenhousz had described the irregular

[1]He uses this as a proof of the existence of atoms: "Observe what happens when sunbeams are admitted into a building and shed light on its shadowy places. You will see a multitude of tiny particles mingling in a multitude of ways... their dancing is an actual indication of underlying movements of matter that are hidden from our sight... It originates with the atoms which move of themselves [i.e. spontaneously]. Then those small compound bodies that are least removed from the impetus of the atoms are set in motion by the impact of their invisible blows and in turn cannon against slightly larger bodies. So the movement mounts up from the atoms and gradually emerges to the level of our

motion of coal dust particles on the surface of alcohol in 1785. Nevertheless Brownian motion is traditionally regarded as discovered by the botanist Robert Brown in 1827. It is believed that Brown was studying pollen particles floating in water under the microscope. He then observed minute particles within the vacuoles of the pollen grains executing a jittery motion. By repeating the experiment with particles of dust, he was able to rule out that the motion was due to pollen particles being 'alive', although the origin of the motion was yet to be explained.

See the film: https://en.wikipedia.org/wiki/Brownian_motion#/media/File:Brownian_motion_large.gif.

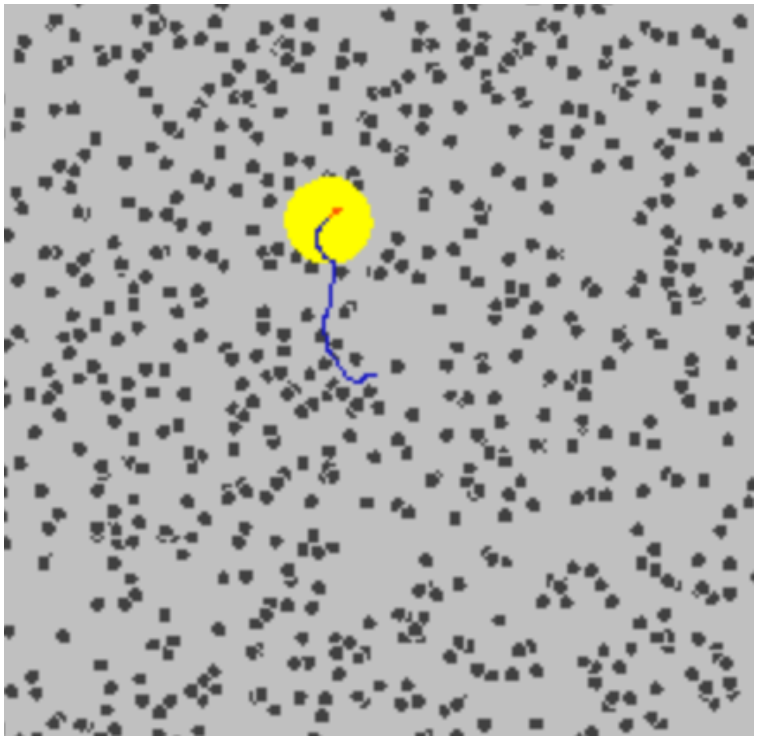

Figure 8.1: Snapshot of a movement of a Brownian particle.

The first person to describe the mathematics behind Brownian motion was Thorvald N. Thiele in 1880 in a paper on the method of least squares. This was followed independently by Louis

senses, so that those bodies are in motion that we see in sunbeams, moved by blows that remain invisible." Although the mingling motion of dust particles is caused largely by air currents, the glittering, tumbling motion of small dust particles is, indeed, caused chiefly by true Brownian dynamics.

Bachelier in 1900 in his PhD thesis "The theory of speculation", in which he presented a stochastic analysis of the stock and option markets. However, it was Albert Einstein's (in his 1905 paper) and Marian Smoluchowski's (1906) independent research of the problem that brought the solution to the attention of physicists, and presented it as a way to indirectly confirm the existence of atoms and molecules. The confirmation of Einstein's theory constituted empirical progress for the kinetic theory of heat. In essence, Einstein showed that the motion can be predicted directly from the kinetic model of thermal equilibrium. The importance of the theory lay in the fact that it confirmed the kinetic theory's account of the second law of thermodynamics as being an essentially statistical law.

8.1 Brownian motion: Statistical description

Einstein's argument was to determine how far a Brownian particle travels in a given time interval. Classical mechanics is unable to determine this distance because of the enormous number of bombardments a Brownian particle will undergo, roughly of the order of 1021 collisions per second. Thus Einstein was led to consider the collective motion of Brownian particles.

He regarded the increment of particle positions in unrestricted one dimensional $x-$ domain as a random variable (Δ or x, under coordinate transformation so that the origin lies at the initial position of the particle) with some probability density function $\phi(\Delta)$. Further, assuming conservation of particle number, he expanded the density (number of particles per unit volume) change

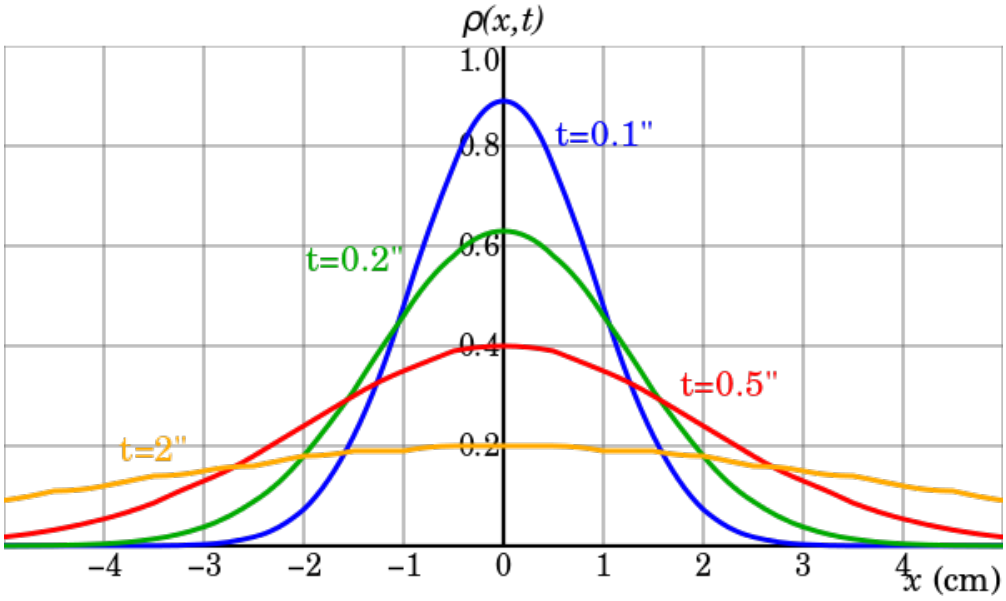

Figure 8.2: The characteristic bell-shaped curves of the diffusion of Brownian particles. The distribution begins as a Dirac delta function, indicating that all the particles are located at the origin at time t=0, and for increasing times they become flatter and flatter until the distribution becomes uniform in the asymptotic time limit.

in a Taylor series:

$$\rho(x, t+\tau) = \rho(x,t) + \tau \frac{\partial \rho(x)}{\partial t} \tag{8.1}$$

$$= \int_{-\infty}^{+\infty} \rho(x+\Delta, t) \cdot \phi(\Delta)\, \mathrm{d}\Delta \tag{8.2}$$

$$= \rho(x,t) \cdot \int_{-\infty}^{+\infty} \phi(\Delta)\, d\Delta + \frac{\partial \rho}{\partial x} \cdot \int_{-\infty}^{+\infty} \Delta \cdot \phi(\Delta)\, \mathrm{d}\Delta$$

$$+ \frac{\partial^2 \rho}{\partial x^2} \cdot \int_{-\infty}^{+\infty} \frac{\Delta^2}{2} \cdot \phi(\Delta)\, \mathrm{d}\Delta \quad + \quad \ldots \tag{8.3}$$

$$= \rho(x,t) \cdot 1 + 0 + \frac{\partial^2 \rho}{\partial x^2} \cdot \int_{-\infty}^{+\infty} \frac{\Delta^2}{2} \cdot \phi(\Delta)\, \mathrm{d}\Delta \quad + \quad \ldots \tag{8.4}$$

The integral in the first term is equal to one by the definition of probability, and the second and

other even terms (i.e. first and other odd moments) vanish because of space symmetry. What is left gives rise to the following relation:

$$\frac{\partial \rho}{\partial t} = \frac{\partial^2 \rho}{\partial x^2} \cdot \int_{-\infty}^{+\infty} \frac{\Delta^2}{2\,\tau} \cdot \phi(\Delta)\,\mathrm{d}\Delta + \textbf{higher order even moments}$$

Where the coefficient before the Laplacian, the second moment of probability of displacement Δ, is interpreted as mass diffusivity D :

$$D = \int_{-\infty}^{+\infty} \frac{\Delta^2}{2\,\tau} \cdot \phi(\Delta)\,\mathrm{d}\Delta$$

Then the density of Brownian particles ρ at point x at time t satisfies the diffusion equation:

$$\frac{\partial \rho}{\partial t} = D \cdot \frac{\partial^2 \rho}{\partial x^2},$$

Assuming that N particles start from the origin at the initial time $t = 0$, the diffusion equation has the solution

$$\rho(x,t) = \frac{N}{\sqrt{4\pi D t}} e^{-\frac{x^2}{4Dt}}.$$

This expression allowed Einstein to calculate the moments directly. The first moment is seen to vanish, meaning that the Brownian particle is equally likely to move to the left as it is to move to the right. The second moment is, however, non-vanishing, being given by

$$\overline{x^2} = 2\,D\,t.$$

This expresses the mean squared displacement in terms of the time elapsed and the diffusivity. From this expression Einstein argued that the displacement of a Brownian particle is not proportional to the elapsed time, but rather to its square root. His argument is based on a conceptual switch from the "ensemble" of Brownian particles to the "single" Brownian particle: we can speak of the relative number of particles at a single instant just as well as of the time it takes a Brownian

particle to reach a given point.

This can be formalized as follows. The Wiener process is a continuous-time stochastic process with stationary independent increments. The Wiener process $\boldsymbol{W_t}$ is characterized by three facts:

- $\boldsymbol{W_0 = 0}$
- $\boldsymbol{W_t}$ is almost surely continuous
- $\boldsymbol{W_t}$ has independent increments with normal distribution $\boldsymbol{W_t - W_{t_0} \sim N(0, t - t_0)}$. $\boldsymbol{N(\mu, \sigma^2)}$ denotes the normal distribution with expected value $\boldsymbol{\mu}$ and variance $\boldsymbol{\sigma^2}$**.** The condition that it has independent increments means that if then and are independent random variables.

The Wiener process can be constructed as the scaling limit of a random walk, or other discrete-time stochastic processes with stationary independent increments. It can be denoted as

$$\boldsymbol{var(W_t) = \overline{dW_t^2} = 2\sigma^2 t} \tag{8.5}$$

where $\boldsymbol{\overline{dW_t^2}}$ is the mean square displacement of a Brownian particle in time $\boldsymbol{t}$ ($\boldsymbol{t_0}$ is set to zero).[2] The so-called diffusion constant $\boldsymbol{D = \sigma^2}$ is related to the mean free path $\boldsymbol{\lambda}$ and the average time between collisions $\boldsymbol{\tau}$:

$$\boldsymbol{2D = \frac{\lambda^2}{\tau}} \quad . \tag{8.6}$$

The time evolution of the position of the Brownian particle itself is best described using Langevin equation, an equation which involves a random force field representing the effect of the thermal fluctuations of the solvent on the particle. The displacement of a particle undergoing Brownian motion is obtained by solving the diffusion equation under appropriate boundary conditions and finding the root mean square of the solution. This shows that the displacement varies as the square

[2] A heuristic helpful interpretation of the stochastic differential equation is that in a small time interval of length $\boldsymbol{dt}$, the stochastic process changes its value by an amount that is normally distributed with variance $\boldsymbol{2\sigma^2 dt}$ and is independent of the past behavior of the process. This is so because the increments of a Wiener process are independent and normally distributed.

root of the time (not linearly).

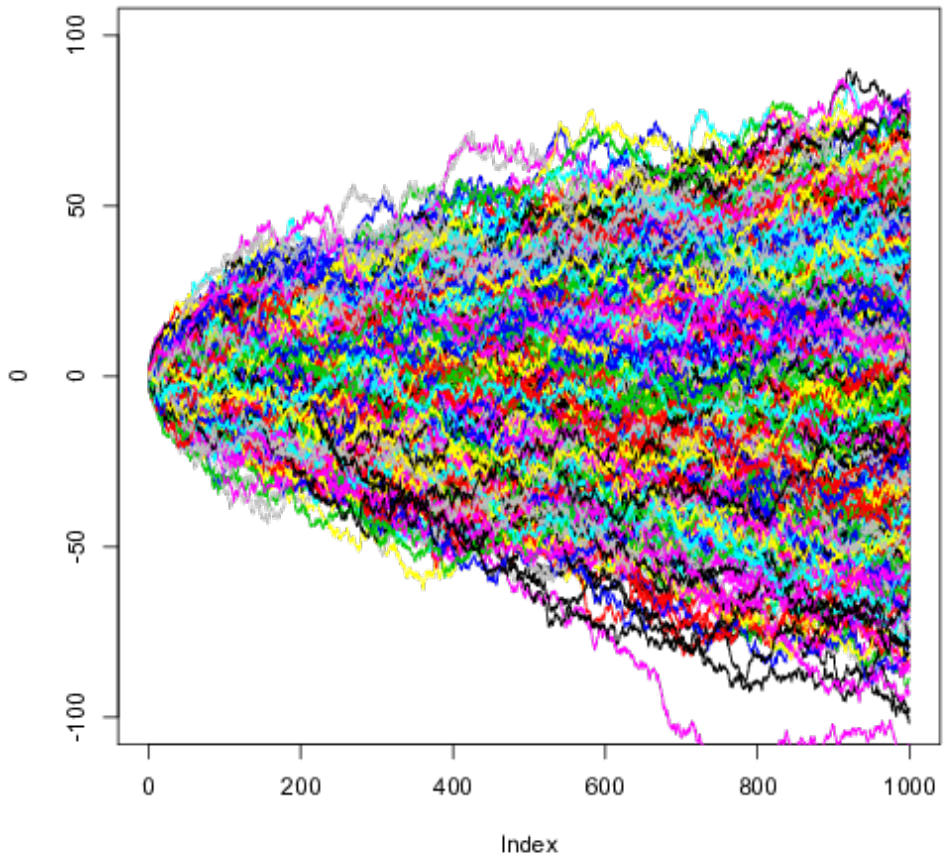

Figure 8.3: Numerical solution of the brownian motion, multiple particles. See exercise 56 for details.

Exercise 56 – Brownian motion on a computer

Imagine a so-called red-noise process

$$\frac{dx}{dt} = -\lambda x + \xi \,. \tag{8.7}$$

1. Calculate the model using the following R code:

```
#brownian motion, multiple particle
#forward modelling

Nparticle<-1000 #number of particles
T<-  1000   #integration time in time units
h<-  0.5   #step size in time units

beta<-0.00001 #friction term
lambda<-1 #noise term

N<-T/h
t<-(0:(N-1))*h

x<-matrix(0,Nparticle,N) # Initial condition, all = 0


for (i in 1:(N-1))
{
  x[,i+1]<-x[,i]*(1-beta*h)+ rnorm(Nparticle)*sqrt(h)

}


plot(0,xlim=c(0,T),ylim=c(-100,100),type="n")
for (i in 1:N) lines (t,x[i,],col=i)

#analyse the densities
h<-matrix(0,N,40)

for (i in 1:(N-1)) h[i,]<-hist(x[,i],breaks=c((-20:20)*10),freq=FALSE,
              ylim=c(0,0.04))$counts

filled.contour(t,(-19:20)*10-5,h,color.palette=rainbow,xlab="time",
              ylab="space")
```

2. Show that the displacement varies as the square root of the time (not linearly).

8.2 Stochastic climate model

In a stochastic framework of climate theory one may use an appropriate stochastic differential equation (Langevin equation)

$$\frac{d}{dt}x(t) = f(x) + g(x)\xi, \tag{8.8}$$

where $\xi = \frac{d}{dt}W(t)$ is a stationary stochastic process and the functions $f, g : \mathbf{R}^n \to \mathbf{R}^n$ describe the climate dynamics. The properties of the random force are described through its distribution and its correlation properties at different times. The process ξ is assumed to have a Gaussian distribution of zero average,

$$< \xi(t) >= 0 \tag{8.9}$$

and to be δ-correlated in time,

$$< \xi(t)\xi(t+\tau) >= \delta(\tau) \tag{8.10}$$

where δ is the delta function defined by

$$\int_{\mathbf{R}} f(x)\,\delta(x - x_0)\,dx = f(x_0) \quad . \tag{8.11}$$

The brackets indicate an average over realizations of the random force.[3] For a Gaussian process only the average and second moment need to be specified since all higher moments can be expressed in terms of the first two. Note that the dependence of the correlation function on the time difference τ assumes that ξ is a stationary process. ξ is called a white-noise process (for the colors of noise: https://en.wikipedia.org/wiki/Colors_of_noise). In general, the stochastic processes can be also described by the probablity distributions (9.19) which will be considered later.

Additionally, there might be an external forcing $F(x,t)$ which is generally time-, variable-, and space-dependent. In his theoretical approach, Hasselmann [1976] formulated a linear stochas-

[3]Formally: $\xi(t)$ is a random variable, i.e. $\xi(t)(\alpha)$ with different realizations due to random variable α. The expectation $< \xi(t) >$ is thus the mean over all $\alpha :< \xi(t)(\alpha) >_\alpha$. Using the ergodic hypothesis, the ensemble average $\langle\rangle$ can be expressed as the time average $\lim_{T\to\infty} \frac{1}{T}\int_{-T/2}^{T/2} dt$ of the function. Almost all points in any subset of the phase space eventually revisit the set. (https://en.wikipedia.org/wiki/Ergodic_theory

tic climate model

$$\frac{d}{dt}x(t) = Ax + \sigma\xi + F(t) \quad , \tag{8.12}$$

with system matrix $A \in \mathbf{R}^{n\times n}$, constant noise term σ, and stochastic process ξ. Many features of the climate system can be well described by (8.12), which is analogous to the Ornstein-Uhlenbeck process in statistical physics [Uhlenbeck and Ornstein, 1930]. Notice that $\sigma\xi$ represents a stationary random process. The relationship derived above is identical to that describing the diffusion of a fluid particle in a turbulent fluid. In a time-scale separated system, during one slow-time unit the fast uninteresting variables y perform many 'uncorrelated' events (provided that the fast dynamics are sufficiently chaotic). The contribution of the uncorrelated events to the dynamics of the slow interesting variables x is as a sum of independent random variables. By the weak central limit theorem this can be expressed by a normally distributed variable. Note, in the absence of any feedback effects Ax, the climate variations would continue to grow indefinitely as the Wiener process.

Numerical integration of the Langevin equation

One can numerically integrate such a nonlinear Langevin equation with flow $f(x)$ using a simple Euler-Maruyama method with a fixed time step Δt :

$$x(t+\Delta t) = x(t) + f(x)\Delta t + g(x)\sqrt{\Delta t}\Delta W_n \tag{8.13}$$

The variables ΔW_n are known as increments of the Wiener process; they are Gaussian numbers generated in an uncorrelated fashion, for example by using a pseudo-random number generator in combination with the Box-Müller algorithm.

```
% calculate sde in matlab\\
%
th = 1;
mu = 1.2;
sig = 0.3;
dt = 1e-2;
t= 0:dt:20;
```

```
x = zeros(1,length(t)); % Allocate output vector, set initial condition
rng(1);                 % Set random seed
for i = 1:length(t)-1
    x(i+1) = x(i)+th*(mu-x(i))*dt+sig*sqrt(dt)*randn;
end
figure;
plot(t,x);
```

and this is for the analytical solution:

```
th = 1;
mu = 1.2;
sig = 0.3;
dt = 1e-2;
t = 0:dt:20;       % Time vector
x0 = 0;           % Set initial condition
rng(1);           % Set random seed
ex = exp(-th*t);
x = x0*ex+mu*(1-ex)+sig*ex.*cumsum([0 sqrt(diff(exp(2*th*t)-1)).
          *randn(1,length(t)-1)])/sqrt(2*th);
figure;
plot(t,x);
```

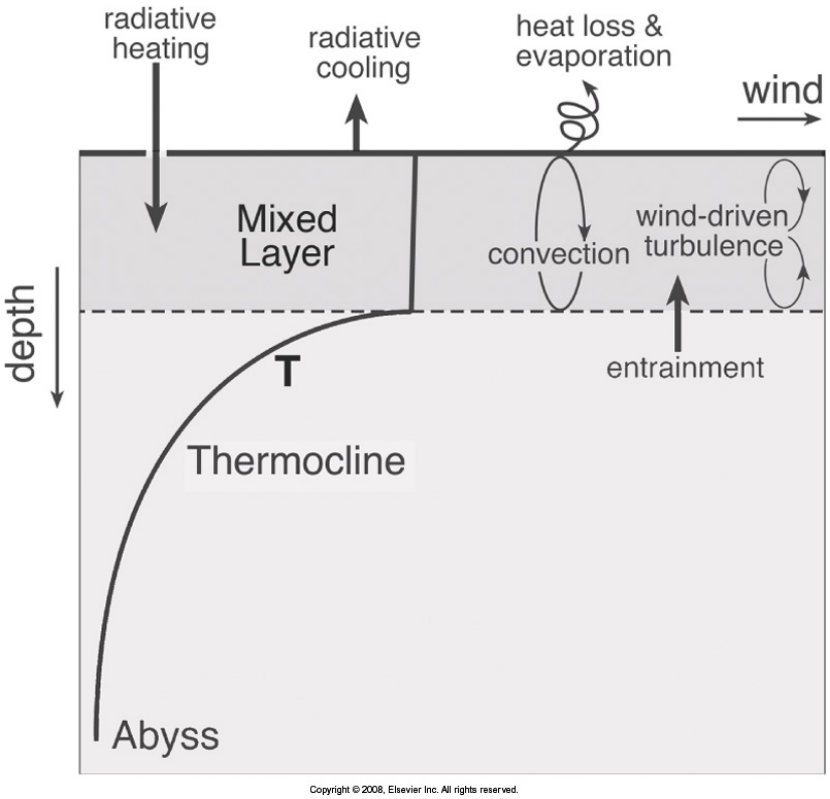

Figure 8.4: Schematic picture of mixed layer in the ocean.

Exercise 57 – Stochastic Climate Model

Imagine that the temperature of the ocean mixed layer of depth h (Fig. 8.4) is governed by

$$\frac{dT}{dt} = -\lambda T + \frac{Q_{net}}{\gamma_O}, \tag{8.14}$$

where coefficient γ_O is given by the heat capacity time density times mixed layer depth $c_p \rho h$. $(h = 100m; c_p = 4.2 \cdot 10^3 Jkg^{-1}K^{-1}; \rho = 1023 kgm^{-3})$. λ is the typical damping rate of a temperature anomaly. Observations show that sea surface temperatures a typically damped at a rate of $15 Wm^{-2}K^{-1}$.

1. Calculate the typical time scale $1/\lambda$.
2. Calculate the stochastic climate model using the R code

```
# Stochastic climate model/Ornstein-Uhlenbeck/Red Noise: Brown.R
T<-  5000   #integration time in time units
h<-  0.1   #step size in time units
X0<- 10     #inital value
beta<-0.05 #friction term
lambda<-1 #noise term
N<-T/h
t<-(0:(N-1))*h

x<-vector()
x[1]<-X0

for (i in 1:(N-1)) {
  x[i+1]<-x[i]*(1-beta*h)+ rnorm(1)*sqrt(h)
}

plot(t,x,type="l")
hist(x,freq=FALSE, col="gray")
```

From the online malterial, please see the browngui directory: BrownianMotion.zip See Figure 8.6.

3. Do the same, but for many Brownian particles in a potential (cf. Fig. 8.7).

```
# Brownian motion, multiple particle: Brown_mult.R
# forward modelling

#the function dy/dt<-f(y,a,b,c,d)
f<-function(y,a,b,c,d)
{ return(d*y^3+c*y^2+b*y-a)    }

#constants
Ca<-10
a<-1
b<- 0.8
c<- 0
d<- -0.001

Nparticle<-1000 #number of particles
T<-  500   #integration time in time units
h<-  0.5   #step size in time units
N<-T/h
t<-(0:(N-1))*h

x<-matrix(10,Nparticle,N) # Initial condition, all = 0
# Initial condition,

for (i in 1:(N-1)) {
  x[,i+1]<- x[,i]+h*f(x[,i],a,b,c,d)  + Ca*rnorm(Nparticle)*sqrt(h)
}

ama2=max(x,2)
ami=min(x,-2)
ama=max(ama2,-ami)
plot(0,xlim=c(0,T),ylim=c(ami,ama),type="n")
for (i in 1:10) lines (t,x[i,],col=i)

#analyse the densities
h<-matrix(0,N,40)
for (i in 1:(N-1)) { h[i,]<-hist(x[,i],breaks=
      c(-20:20)*ama/10,freq=FALSE,ylim=c(0,0.04))$counts    }
hstat<-matrix(0,N)
for (i in N/2:(N-1)) hstat[]<-h[i,]+hstat[]
hstat[]<-hstat[] *2/Nparticle/N
#plot(t,hstat[],type="l")
plot(table(hstat[]), type = "h", col = "red")

# to show the time evolution, 1, 2, 4, 8, ....  time step
 op <- par(mfrow = c(3, 2))
plot(h[1,]/Nparticle,type="l")
plot(h[2,]/Nparticle,type="l")
plot(h[4,]/Nparticle,type="l")
plot(h[8,]/Nparticle,type="l")
plot(h[N/2,]/Nparticle,type="l")
```

```
plot(h[N-1,]+h[N-2,]/Nparticle/2,type="l")

filled.contour(t,(-19:20)*ama/10-ama/20,h,
      color.palette=rainbow,xlab="time",ylab="space")
```

4. Calculate the stationary density from the numerical example analytically using $\int \boldsymbol{f}(\boldsymbol{y})\boldsymbol{dy}$.

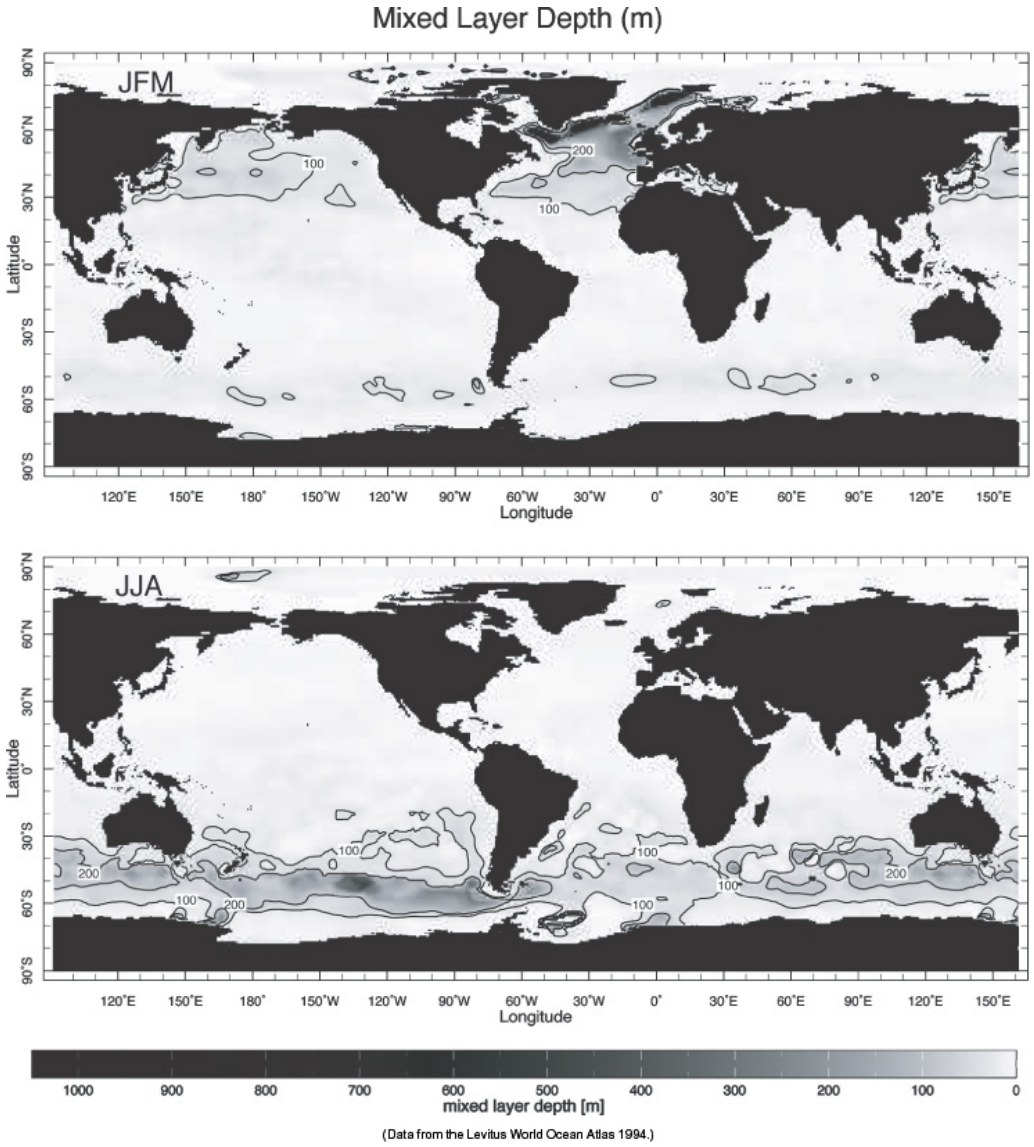

Figure 8.5: Mixed layer in the ocean distribution. Task: Describe the distribution of the seasonal mixed layer depth variations!

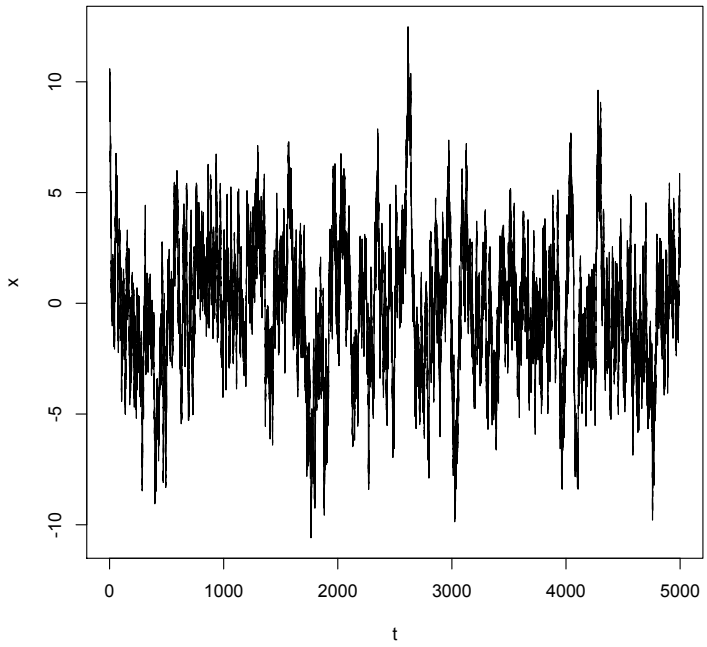

Figure 8.6: Stochastic Climate model, see (8.43).

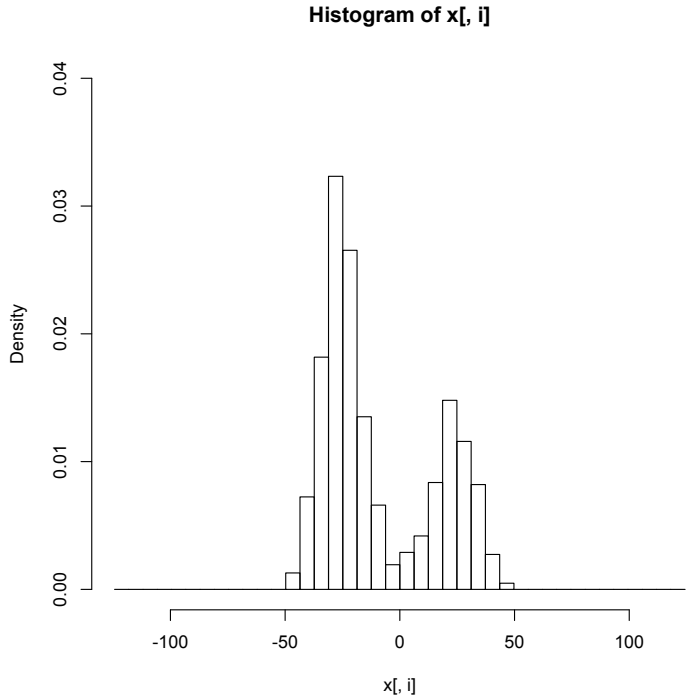

Figure 8.7: Histogram: Stochastic Climate model in potential

An important example is the equation for geometric Brownian motion

$$\mathrm{d}\boldsymbol{X}_t = \boldsymbol{\mu}\boldsymbol{X}_t\,\mathrm{d}\boldsymbol{t} + \boldsymbol{\sigma}\boldsymbol{X}_t\,\mathrm{d}\boldsymbol{W}_t. \tag{8.15}$$

which is the equation for the dynamics of the price of a stock in the Black Scholes options pricing model of financial mathematics. For an arbitrary initial value $\boldsymbol{X_0}$ the above SDE has the analytic solution (https://en.wikipedia.org/wiki/Geometric_Brownian_motion):

$$\boldsymbol{X}_t = \boldsymbol{X}_0 \exp\left(\left(\boldsymbol{\mu} - \frac{\boldsymbol{\sigma}^2}{\boldsymbol{2}}\right)\boldsymbol{t} + \boldsymbol{\sigma}\boldsymbol{W}_t\right). \tag{8.16}$$

which is shown in Fig. 8.8.

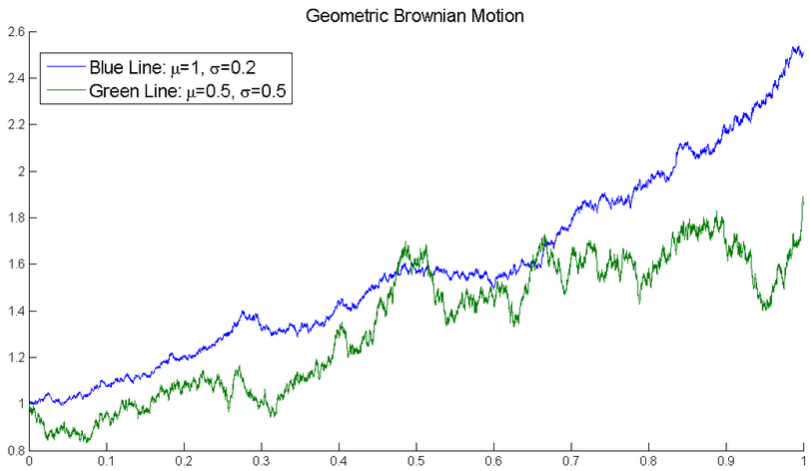

Figure 8.8: Two sample paths of Geometric Brownian motion, with different parameters. The blue line has larger drift, the green line has larger variance.

Exercise 58 – Stochastic Stock market Model

1. Solve equation (8.16) in a similar way as exercise 57!
2. Why is $\boldsymbol{X_t}$ always positive?
3. Calculate the stationary density from the numerical example analytically using $\int \boldsymbol{f(y)dy}$.

Exercise 59 – Spectrum of Stochastic Climate Model

Imagine that the temperature of the ocean mixed layer of depth h is governed by

$$\frac{dT}{dt} = -\lambda T + \frac{Q_{net}}{\gamma_O}, \tag{8.17}$$

where coefficient γ_O is given by the heat capacity $c_p \rho h$, and λ is the typical damping rate of a temperature anomaly. The air-sea fluxes due to weather systems are represented by a white-noise process $Q_{net} = \hat{Q}_\omega e^{i\omega t}$ where $\hat{Q}_\omega$ is the amplitude of the random forcing at frequency ω and $\hat{Q}^*$ is the complex conjugate. Remember that Q_{net} can be described through its distribution and its correlation properties: a Gaussian distribution of zero average $< Q_{net} >= 0$ and δ-correlated in time $< Q_{net}(t) Q_{net}(t+\tau) >= \delta(\tau)$ The brackets indicate an average over realizations of the random force. The spectrum of a process x is defined as

$$S(\omega) \;:=\; \langle \hat{x}\hat{x}^* \rangle = \widehat{Cov_x(\tau)} \;= \int_R \exp(i\omega\tau) Cov_x(\tau) d\tau \tag{8.18}$$

1. Calculate $S_Q(\omega)$ and describe why Q_{net} is called a white noise process.
2. Solve Eq. 8.17 for the temperature response $T = \hat{T}_\omega e^{i\omega t}$ and hence show that:

$$\hat{T}_\omega = \frac{\hat{Q}_\omega}{\gamma_O (\lambda + i\omega)} \tag{8.19}$$

3. Show that it has a spectral density $\hat{T}_\omega \hat{T}^*_\omega$ is given by:

$$\hat{T}\hat{T}^* = \frac{\hat{Q}\hat{Q}^*}{\gamma_O^2 (\lambda^2 + \omega^2)} \tag{8.20}$$

and the spectrum

$$S(\omega) =< \hat{T}\hat{T}^* >= \frac{1}{\gamma_O^2 (\lambda^2 + \omega^2)}. \tag{8.21}$$

The brackets $< \cdots >$ denote the ensemble mean. Make a sketch of the spectrum using a

log-log plot and show that fluctuations with a frequency greater than λ are damped.

4. Calculate the spectrum of a regular oszillation with noise. How does the spectrum changes when you rectify the signal?

```
a<-sin(2*pi*(1:5000)/20)+0.5*rnorm(5000)/10
plot(a,type="l",xlim = c(0,2*pi*20),xlab='time (kyrs)',ylab='forcing')
b<-pmax(-0.1,a)  # rectify the signal
plot(b,type="l",col="red",xlim=c(0,2*pi*20),
  xlab='time (kyrs)',ylab='climate')
sa<-spectrum(a,spans=10,
  main="Spectrum of forcing (spans=10)",col="blue")
sb<-spectrum(b,spans=10, col="red")
plot(sa,col="blue",main="Spectrum of the rectified signal (spans=10)")
plot(sb,add = TRUE, col = "red")
```

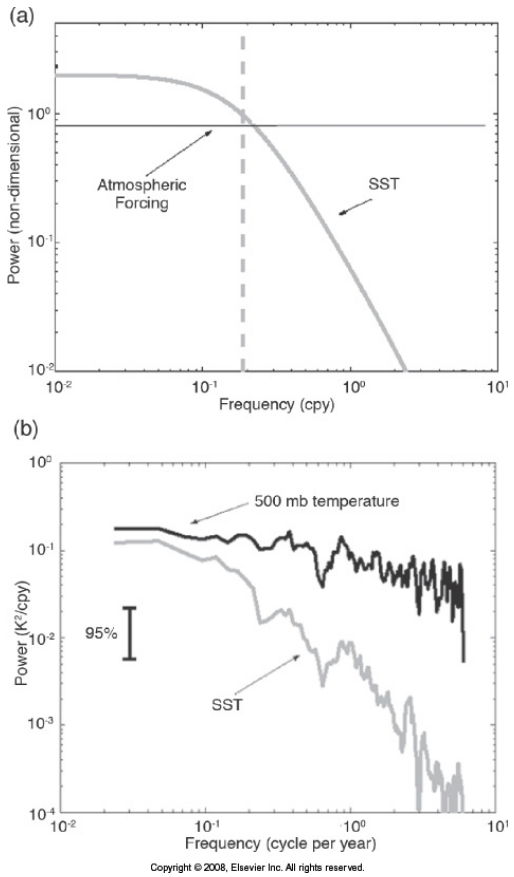

Figure 8.9: Powerspectrum of atmospheric temperature and sea surface temperature. Here $1/\lambda = 300$ days from equation (8.43).

Exercise 60 – Climate sensitivity and variability in the Stochastic Climate Model

As in exercise 59, imagine that the temperature of the ocean mixed layer of depth h is governed by

$$\frac{dT}{dt} = -\lambda T + Q_{net} + f(t)\,, \tag{8.22}$$

where the air-sea fluxes due to weather systems are represented by a white-noise process with zero average $< Q_{net} >= 0$ and δ-correlated in time $< Q_{net}(t)Q_{net}(t+\tau) >= \delta(\tau)$. The function $f(t)$ is a time dependent deterministic forcing. Assume furthermore that $f(t) = c \cdot u(t)$ with $u(t)$ as unit step or the so-called Heaviside step function and solve (8.22). What is the relationship of the dissipation (through λ) and the fluctuations (through the spectrum $S(\omega)$) ?

Solution

Since $Q(t)$ is a stochastic process, it has to be solved for the moments. Because $< Q_{net} >= 0$, $< T(t) >$ can be solved using the Laplace transform:

$$< T(t) > = \mathcal{L}^{-1}\{F(s)\}(t) = \mathcal{L}^{-1}\left\{\frac{< T(0) >}{s+\lambda} + \frac{c}{s}\cdot\frac{1}{s+\lambda}\right\} \tag{8.23}$$

$$= T(0)\cdot\exp(-\lambda t) + \frac{c}{\lambda}\left(1-\exp(-\lambda t)\right) \tag{8.24}$$

because we have $< T(0) >= T(0)$. As equilibrium response, we have

$$\Delta T = \lim_{t\to\infty} < T(t) >= \frac{c}{\lambda}\,. \tag{8.25}$$

The fluctuation can be characterized by the spectrum (exercise 59)

$$S(\omega) =< \hat{T}\hat{T}^{*} >= \frac{1}{\lambda^2+\omega^2}. \tag{8.26}$$

and therefore, the spectrum and the equilibrium response are closely coupled (fluctuation-dissipation theorem).

For some energy considerations, it is usefull to re-write equation (8.22) as

$$C\,\frac{dT}{dt} = -\lambda_C T + f_C\,, \tag{8.27}$$

with $C = c_p \rho dz$ as the heat capacity of the ocean. For a depth of 200 m of water distributed over the globe, $C = 4.2{\cdot}10^3 Ws\,kg^{-1}K^{-1} \times 1000\,kg\,m^{-3} \times 200\,m = 8.4{\cdot}10^8\,Ws\,m^{-2}\,K^{-1}$. The temperature evolution is

$$T(t) = T(0)\cdot \exp(-\lambda_c/C\,t)\; + \;\frac{f_C}{\lambda_C}\,(1-\exp(-\lambda_C/C\,t)) \tag{8.28}$$

The left hand side of (8.27) represents the heat uptake by the ocean, which plays a central role in the transient response of the system to a perturbation (8.28).

Typical changes in f_C are $4\,Wm^{-2}$ for doubling of CO_2, $\lambda_C = 1-2\,Wm^{-2}K^{-1}$. The typical time scale for a mixed layer ocean is $C/\lambda_C = 13-26$ years . Please note that the climate system is simplified by a slab ocean with homogenous temperature and heat capacity. This is an approximation as the heat capacity should vary in time as the perturbation penetrates to deeper oceanic levels.

The equilibrium temperature change ΔT is

$$\Delta T = \frac{\Delta f_C}{\lambda_C} = \frac{c}{\lambda} \tag{8.29}$$

with values of $\Delta T = 2-4$ K. The term $CS = \frac{1}{\lambda_C}$ is called climate sensitivity to a radiative forcing Δf_C:

$$\Delta T = CS \;\cdot\; \Delta f_C \quad . \tag{8.30}$$

In the literature, the concept of climate sensitivity is quite often used as the equilibrium temperature increase for a forcing Δf_C related to doubling of CO_2.

Exercise 61 – Stochastic differential equation

Tasks:

1. Simulate the velocity evolution of one particle which is determined by the following stochastic $dv/dt = -b * v + k * dW(t)/dt$
2. What happens if you change the timestep?
3. Simulate the ensemble of multiple particles, plot the time evolution of the v-Distribution
4. Test the ergodic theorem: time average = ensemble average

Solution

```
#brownian motion, one particle

T<-  5000   #integration time in time units
h<-  0.1   #step size in time units
X0<- 10     #inital value

beta<-0.05 #friction term
lambda<-1 #noise term

N<-T/h
t<-(0:(N-1))*h

x<-vector()
x[1]<-X0

for (i in 1:(N-1))
{
  x[i+1]<-x[i]*(1-beta*h)+ rnorm(1)*sqrt(h)
}

plot(t,x,type="l")
# dev.print(postscript, file="random.ps")
#hist(x)
#hist(x,freq=FALSE, col="gray")
```

Solution brownian motion, multiple particle

```
#brownian motion, multiple particle
#forward modelling

#the function dy/dt<-f(y,a,b,c,d)
# double well potential
```

```
f<-function(y,a,b,c,d)
{
  return(d*y^3+c*y^2+b*y-a)
}



#constants
Ca<-10  # noise

a<-1
b<- 0.8
c<- 0
d<- -0.001

# to do: caculate the stationary density analytically:  int 2/Ca f(y) dy

Nparticle<-1000 #number of particles
T<-  1000   #integration time in time units
h<-  0.5   #step size in time units

N<-T/h
t<-(0:(N-1))*h

x<-matrix(10,Nparticle,N) # Initial condition, all = 0
#x<-matrix(rnorm(Nparticle)*10,Nparticle,N) # Initial condition,

for (i in 1:(N-1))
{
  x[,i+1]<- x[,i]+h*f(x[,i],a,b,c,d)  + Ca*rnorm(Nparticle)*sqrt(h)
}

ama2=max(x,2)
ami=min(x,-2)
ama=max(ama2,-ami)

plot(0,xlim=c(0,T),ylim=c(ami,ama),type="n")  # frame
#plot(0,xlim=c(0,T),ylim=c(-100,100),type="n") # with fixed ylim

# plot the realizations in different colors
for (i in 1:10) lines (t,x[i,],col=i)


#analyse the densities: time evolution
h<-matrix(0,N,40)
#for (i in 1:(N-1)) h[i,]<-hist(x[,i],breaks=c((-20:20)*10),
#             plot=FALSE)$counts

for (i in 1:(N-1)) h[i,]<-hist(x[,i],breaks=c(-20:20)*ama/10,
          freq=FALSE,ylim=c(0,0.04))$counts

#hstat<-matrix(0,N)
```

```
#for (i in N/2:(N-1)) hstat[]<-h[i,]+hstat[]
#hstat[]<-hstat[] *2/Nparticle/N
#plot(t,hstat[],type="l")
 plot(table(hstat[]), type = "h", col = "red")

 op <- par(mfrow = c(3, 2))
plot(h[1,]/Nparticle,type="l")
plot(h[2,]/Nparticle,type="l")
plot(h[4,]/Nparticle,type="l")
plot(h[8,]/Nparticle,type="l")
plot(h[N/2,]/Nparticle,type="l")
plot(h[N-1,]+h[N-2,]/Nparticle/2,type="l")


#filled.contour(t,(-19:20)*10-5,h,color.palette=rainbow,xlab="time",
#              ylab="space")

filled.contour(t,(-19:20)*ama/10-ama/20,h,color.palette=rainbow,
              xlab="time",ylab="space")

#dev.print(postscript, file="/tmp/out.ps")
# system("lpr -Pps3 /tmp/out.ps")
```

8.3 Sprectral methods

8.3.1 Fourier transform

The Fourier transform decomposes a function of time (e.g., a signal) into the frequencies that make it up, similarly to how a musical chord can be expressed as the amplitude (or loudness) of its constituent notes. The Fourier transform of a function of time itself is a complex-valued function of frequency, whose absolute value represents the amount of that frequency present in the original function, and whose complex argument is the phase offset of the basic sinusoid in that frequency. The Fourier transform is called the frequency domain representation of the original signal. The term Fourier transform refers to both the frequency domain representation and the mathematical operation that associates the frequency domain representation to a function of time (see also https://en.wikipedia.org/?title=Fourier_transform).

The Fourier transformation of $\boldsymbol{x}$ is defined as

$$\hat{\boldsymbol{x}}(\boldsymbol{\omega}) = \int_{\mathbf{R}} \boldsymbol{x}(\boldsymbol{t}) \boldsymbol{e}^{i\omega t}\, \boldsymbol{dt} \tag{8.31}$$

and is denoted as a hat in the following.[4] And the inverse Fourier transformation of $\boldsymbol{x}$ is defined as

$$\boldsymbol{x}(\boldsymbol{t}) = \frac{\mathbf{1}}{\mathbf{2\pi}} \int_{\mathbf{R}} \hat{\boldsymbol{x}}(\boldsymbol{\omega}) \boldsymbol{e}^{-i\omega t}\, \boldsymbol{d\omega} \tag{8.32}$$

or with $\boldsymbol{\omega} = \mathbf{2\pi\nu}$:

$$\boldsymbol{x}(\boldsymbol{t}) = \int_{\mathbf{R}} \hat{\boldsymbol{x}} \boldsymbol{e}^{-i2\pi\nu t}\, \boldsymbol{d\nu} \quad . \tag{8.33}$$

[4] Other common notations for the Fourier transform $\hat{\boldsymbol{x}}(\boldsymbol{\omega})$: $\tilde{\boldsymbol{x}}(\boldsymbol{\omega})$, $\tilde{\boldsymbol{x}}(\boldsymbol{\omega})$, $\boldsymbol{F}(\boldsymbol{\xi})$, $\boldsymbol{\mathcal{F}}\,(\boldsymbol{x})\,(\boldsymbol{\omega})$, $(\boldsymbol{\mathcal{F}x})\,(\boldsymbol{\omega})$, $\boldsymbol{\mathcal{F}}(\boldsymbol{x})$, $\boldsymbol{\mathcal{F}}(\boldsymbol{\omega})$, $\boldsymbol{F}(\boldsymbol{\omega})$. The sign of the exponential in the Fourier transform is something that we are concerned with for many years. Of course, there are two conventions that have been used with almost equal frequency, but I try to stick to one of them to avoid confusion. Here, we have used the convention of the positive sign in the exponential for the forward transform which represents the Fraunhofer diffraction pattern for a real-space object. This is consistent with assuming that a plane wave, going in positive direction in real space is written $\mathbf{exp}\,[\boldsymbol{i}(\boldsymbol{\omega t} - \boldsymbol{kx})]$ rather than a minus sign before the i, so that the phase advances with time.

Exercise 62 – Fourier transformation

Tasks: Calculate the Fourier transformation of

1. $x(t+a)$ (time shift).
2. $x(t*a)$ (Scaling in the time domain).
3. $\frac{d}{dt}x(t)$ (time derivative).
4. $x(t) = \exp(-at^2)$ (Gaussian).
5. $x(t) = \delta(t)$ where the δ distribution is definedthrough the operator on any function y: $y(t_0) = \int_{\mathsf{R}} y(t)\delta(t-t_0)\ dt$
6. Show that for $x(t) = \exp(-iat)$, the Fourier transformation $\hat{x}(\omega) = 2\pi\delta(\omega - a)$. Hint: use the Fourier back transformation (8.31).
7. Calculate the Fourier transformation of a the periodic function $x(t) = \sin(\omega_0 t)$. Remember that $\sin x = \frac{1}{2i}\left(e^{ix} - e^{-ix}\right)$.
8. Prove the Uncertainty principle: the more concentrated $x(t)$ is, the more spread out its Fourier transform $\hat{x}(\omega)$ must be. In particular, the scaling property of the Fourier transform may be seen as saying: if we "squeeze" a function in t, its Fourier transform "stretches out" in ω. It is not possible to arbitrarily concentrate both a function and its Fourier transform.
9. Consider the sine and cosine transforms and show the following. Fourier's original formulation of the transform did not use complex numbers, but rather sines and cosines. Statisticians and others still use this form. An absolutely integrable function f for which Fourier inversion holds good can be expanded in terms of genuine frequencies (avoiding negative frequencies, which are sometimes considered hard to interpret physically) λ by

$$f(t) = \int_0^\infty [a(\lambda)\cos 2\pi\lambda t + b(\lambda)\sin 2\pi\lambda t]\, d\lambda. \tag{8.34}$$

This is called an expansion as a trigonometric integral, or a Fourier integral expansion. The coefficient functions a and b can be found by using variants of the Fourier cosine transform

and the Fourier sine transform (the normalisations are, again, not standardised):

$$a(\lambda) = 2\int_{-\infty}^{\infty} f(t)\cos(2\pi\lambda t)dt \tag{8.35}$$

$$b(\lambda) = 2\int_{-\infty}^{\infty} f(t)\sin(2\pi\lambda t)dt. \tag{8.36}$$

Laplace transform

The Fourier transform is intimately related with the Laplace transform $F(s)$, which is also used for the solution of differential equations and the analysis of filters (https://en.wikipedia.org/wiki/Laplace_transform). We introduce the complex variable $s = -i\omega$.

$$\mathcal{L}\{x(t)\} = F(s) = \int_0^{\infty} e^{-st}x(t)dt \tag{8.37}$$

It follows (integration by parts for 8.38)

$$\mathcal{L}\left\{\frac{d}{dt}x(t)\right\} = sF(s) - x(0) \tag{8.38}$$

$$\mathcal{L}\{\exp(-at)\} = \frac{1}{s+a} \tag{8.39}$$

$$\mathcal{L}\{-\exp(-at)+\exp(-bt)\} = \frac{-1}{s+a} + \frac{1}{s+b} = \frac{a-b}{(s+a)}\frac{1}{(s+b)} \tag{8.40}$$

The Laplace transform of a sum is the sum of Laplace transforms of each term.

$$\mathcal{L}\{f(t)+g(t)\} = \mathcal{L}\{f(t)\} + \mathcal{L}\{g(t)\} \tag{8.41}$$

The Laplace transform of a multiple of a function is that multiple times the Laplace transformation

Function	Time domain $f(t) = \mathcal{L}^{-1}\{F(s)\}$	Laplace s-domain $F(s) = \mathcal{L}\{f(t)\}$
unit impulse	$\delta(t)$	1
delayed impulse	$\delta(t-\tau)$	$e^{-\tau s}$
unit step	$u(t)$	$\frac{1}{s}$
delayed unit step	$u(t-\tau)$	$\frac{1}{s}e^{-\tau s}$
exponential decay	$e^{-\alpha t} \cdot u(t)$	$\frac{1}{s+\alpha}$
sine	$\sin(\omega t) \cdot u(t)$	$\frac{\omega}{s^2+\omega^2}$
cosine	$\cos(\omega t) \cdot u(t)$	$\frac{s}{s^2+\omega^2}$
decaying sine wave	$e^{-\alpha t}\sin(\omega t) \cdot u(t)$	$\frac{\omega}{(s+\alpha)^2+\omega^2}$
decaying cosine wave	$e^{-\alpha t}\cos(\omega t) \cdot u(t)$	$\frac{s+\alpha}{(s+\alpha)^2+\omega^2}$
natural logarithm	$\ln(t) \cdot u(t)$	$-\frac{1}{s}\left[\ln(s) + \gamma\right]$
Convolution	$(f * g)(t) = \int_0^t f(\tau)g(t-\tau)\,d\tau$	$F(s) \cdot G(s)$

Table 8.1: Laplace transformation (https://en.wikipedia.org/wiki/Laplace_transform.

of that function.

$$\mathcal{L}\{af(t)\} = a\mathcal{L}\{f(t)\} \tag{8.42}$$

Using this linearity, and various trigonometric, hyperbolic, and complex number (etc.) properties and/or identities, some Laplace transforms can be obtained from others quicker than by using the definition directly.

Exercise 63 – Laplace transformation of mixed layer model

Solve the Imagine that the temperature of the ocean mixed layer is governed by

$$\frac{dT}{dt} = -\lambda T + Q(t)\,, \tag{8.43}$$

where λ is the typical damping rate of a temperature anomaly and $Q(t)$ a forcing.

1. Use the Laplace transformation to show

$$F(s) = \frac{Q(s) + T(0)}{s + \lambda} \quad . \tag{8.44}$$

   where $Q(s) = \mathcal{L}\{Q(t)\}$

2. Consider the special case $Q(t) = \exp(i\omega_0 t)$, then $Q(s) = \frac{1}{s - i\omega_0}$. The forcing and the temperature is of course a real number, by representing is as a complex number we can simultaneously keep track of both phase components. Show

$$F(s) = \frac{T(0) + Q(s)}{s + \lambda} = \frac{T(0)}{s + \lambda} + \frac{1}{(s + \lambda)} \frac{1}{(s - i\omega_0)} \tag{8.45}$$

   and via the Laplace back-transformation and (8.39, 8.40) that

$$T(t) = \exp(-\lambda t) T(0) + \frac{[\exp(i\omega_0 t) - \exp(-\lambda t)]}{\lambda + i\omega_0} \quad . \tag{8.46}$$

3. Calculate the real and complex part of (8.46).
4. Show: At low frequencies, the output is equal to the input. At high frequencies it rolls off as $1/\omega$ (it is a low-pass filter) and is out of phase by $90°$.

Let $x(t)$ be the input to a general linear time-invariant system, and $y(t)$ be the output, and the Laplace transform of $x(t)$ and $y(t)$ be $X(s)$ and $Y(s)$. Then, the output is related to the input by convolution with respect to the impulse response $h(t)$ by

$$y(t) = \int_0^\infty h(t') x(t - t') dt \tag{8.47}$$

Because of the convolution, the transfer function $H(s)$ is equal to the to the ratio of the Laplace

transforms of the input and output

$$\boldsymbol{H(s) = \frac{Y(s)}{X(s)}.} \tag{8.48}$$

The impulse response of a linear transformation is the image of Dirac's delta function under the transformation, analogous to the fundamental solution of a partial differential operator. The general feature of the transfer function is that is the ratio of two polynomials. Since the polynomials can be constructed from knowledge of the roots, the location of the poles and zeros completetly characterizes the response of the system. The system is globally stable if all poles lie in the left half-plane with Re(poles) < 0. For example $\boldsymbol{\mathcal{L}\{\exp(-at)\} = \frac{1}{s+a}}$, i.e. the system is stable if $\boldsymbol{Re(a) < 0}$. Poles off the real axes are associated with oscillations. Summarizing, the convolution that gives the output of the system can be transformed to a multiplication in the transform domain, given signals for which the transforms exist

$$\boldsymbol{y(t) = (h * x)(t) \overset{\text{def}}{=} \int_{-\infty}^{\infty} h(t-\tau)x(\tau)\,\mathrm{d}\tau \overset{\text{def}}{=} \mathcal{L}^{-1}\{H(s)X(s)\}.} \tag{8.49}$$

Transfer functions are commonly used in the analysis of systems such as single-input single-output filters, typically within the fields of signal processing, communication theory, and control theory. The term is often used exclusively to refer to linear, time-invariant systems. The descriptions below are given in terms of a complex variable, $\boldsymbol{s = \sigma - i\omega}$, which bears a brief explanation. In many applications, it is sufficient to define $\boldsymbol{\sigma = 0}$, which reduces the Laplace transforms with complex arguments to Fourier transforms with real argument $\boldsymbol{\omega}$. The applications where this is common are ones where there is interest only in the steady-state response.[5] The stability of linear systems will be discussed further in section **??**.

[5] In discrete-time systems, the relation between an input signal x(t) and output y(t) is dealt with using the z-transform, and then the transfer function is similarly written as $\boldsymbol{H(z) = \frac{Y(z)}{X(z)}}$ and this is often referred to as the pulse-transfer function.

Exercise 64 – Method of partial fraction expansion

Consider a linear time-invariant system with transfer function

$$\boldsymbol{H(s) = \frac{1}{(s+\alpha)(s+\beta)}.} \tag{8.50}$$

The impulse response is simply the inverse Laplace transform of this transfer function:

$$\boldsymbol{h(t) = \mathcal{L}^{-1}\{H(s)\}.} \tag{8.51}$$

To evaluate this inverse transform, we begin by expanding $\boldsymbol{H(s)}$ using the method of partial fraction expansion:

$$\boldsymbol{\frac{1}{(s+\alpha)(s+\beta)} = \frac{P}{s+\alpha} + \frac{R}{s+\beta}.} \tag{8.52}$$

The unknown constants P and R are the residues located at the corresponding poles of the transfer function. Each residue represents the relative contribution of that singularity to the transfer function's overall shape. By the residue theorem, the inverse Laplace transform depends only upon the poles and their residues. To find the residue P, we multiply both sides of the equation by $\boldsymbol{s+\alpha}$ to get

$$\boldsymbol{\frac{1}{s+\beta} = P + \frac{R(s+\alpha)}{s+\beta}.} \tag{8.53}$$

Then by letting $\boldsymbol{s = -\alpha}$, the contribution from R vanishes and all that is left is

$$\boldsymbol{P = \left.\frac{1}{s+\beta}\right|_{s=-\alpha} = \frac{1}{\beta-\alpha}.} \tag{8.54}$$

Similarly, the residue R is given by

$$\boldsymbol{R = \left.\frac{1}{s+\alpha}\right|_{s=-\beta} = \frac{1}{\alpha-\beta}.} \tag{8.55}$$

Note that

$$R = \frac{-1}{\beta - \alpha} = -P \tag{8.56}$$

and so the substitution of R and P into the expanded expression for H(s) gives

$$H(s) = \left(\frac{1}{\beta - \alpha}\right) \cdot \left(\frac{1}{s + \alpha} - \frac{1}{s + \beta}\right). \tag{8.57}$$

Finally, using the linearity property and the known transform for exponential decay (see in the Table 8.1 of Laplace transforms, above), we can take the inverse Laplace transform of H(s) to obtain:

$$h(t) = \mathcal{L}^{-1}\{H(s)\} = \frac{1}{\beta - \alpha}\left(e^{-\alpha t} - e^{-\beta t}\right), \tag{8.58}$$

which is the impulse response of the system. (This example will be used in section **??** with more details of the Laplace transformation.)

Exercise 65 – Convolution

The same result can be achieved using the convolution property as if the system is a series of filters with transfer functions of $1/(s + a)$ and $1/(s + b)$. That is, the inverse of

$$H(s) = \frac{1}{(s + a)(s + b)} = \frac{1}{s + a} \cdot \frac{1}{s + b} \tag{8.59}$$

is

$$\mathcal{L}^{-1}\left\{\frac{1}{s + a}\right\} * \mathcal{L}^{-1}\left\{\frac{1}{s + b}\right\} \tag{8.60}$$

$$= e^{-at} * e^{-bt} = \int_0^t e^{-ax} e^{-b(t-x)}\, dx \tag{8.61}$$

$$= \frac{e^{-at} - e^{-bt}}{b - a}. \tag{8.62}$$

An integral formula for the inverse Laplace transform, is given by the line integral:

$$x(t) = \mathcal{L}^{-1}\{F(s)\}(t) = \frac{1}{2\pi i}\lim_{T\to\infty}\int_{\gamma-iT}^{\gamma+iT} e^{st}F(s)\,ds, \tag{8.63}$$

where the integration is done along the vertical line $Re(s) = \gamma$ in the complex plane such that γ is greater than the real part of all singularities of F(s). This ensures that the contour path is in the region of convergence. If all singularities are in the left half-plane, or F(s) is a smooth function on $-\infty < Re(s) < \infty$ (i.e., no singularities), then γ can be set to zero and the above inverse integral formula above becomes identical to the inverse Fourier transform.(https://en.wikipedia.org/wiki/Residue_theorem). The function f(t)=INVLAP(F(s)) offers a simple, effective and reasonably accurate way to achieve the result.[6] The transform F(s) may be any reasonable function of complex variable s^{α}, where α is an integer or non-integer real exponent. Thus, the function INVLAP can solve even fractional problems and invert functions F(s) containing rational, irrational or transcendental expressions. The function does not require to compute poles nor zeroes of F(s). It is based on values of F(s) for selected complex values of the independent variable s. The resultant computational error can be held arbitrarily low at the cost of CPU time (see Examples).

Here is the matlab code for the Numerical Inversion of Laplace Transforms with some examples 0, 1, 2

8.3.2 Covariance and spectrum

A stationary process exhibits an autocovariance function of the form

$$Cov(\tau) = \langle (x(t+\tau) - \langle x\rangle)(x(t) - \langle x\rangle)\rangle \tag{8.64}$$

[6] It is based on the paper: J. Valsa and L. Brancik: Approximate Formulae for Numerical Inversion of Laplace Transforms, Int. Journal of Numerical Modelling: Electronic Networks, Devices and Fields, Vol. 11, (1998), pp. 153-166.

where $\langle \ldots \rangle$ denotes the statistical ensemble mean.[7] Normalized to the variance (i.e. the autocovariance function at $\tau = 0$) one gets the autocorrelation function $C(\tau)$:

$$C(\tau) = Cov(\tau)/Cov(0) \quad . \tag{8.65}$$

Many stochastic processes in nature exhibit short-range correlations, which decay exponentially:

$$C(\tau) \sim \exp(-\tau/\tau_0), \text{ for } \tau \to \infty \tag{8.66}$$

These processes exhibit a typical time scale τ_0. For a white noise process ξ (as defined in 8.10), the autocorrelation function $C(\tau)$ is given by

$$C(\tau) = \delta(\tau) \quad . \tag{8.67}$$

Spectrum of the stochastic process

The Fourier transformation of the random variable x is

$$\hat{x}(\omega) = \int_{\mathsf{R}} x(t) e^{i\omega t}\, dt \quad = \lim_{T\to\infty} \int_{-T/2}^{T/2} x(t) e^{i\omega t}\, dt \tag{8.68}$$

and is also a ramdom variable, but its power spectral density $S(\omega)$ is not:

$$S(\omega) \;:=\; \left\langle \hat{x}\hat{x}^{+} \right\rangle = \left\langle |\hat{x}(\omega)|^2 \right\rangle \quad . \tag{8.69}$$

Using the **ergodic hypothesis**, the ensemble average $S(\omega) = \langle\, \hat{x}\hat{x}^{+} \,\rangle$ can be expressed as the time average

$$\lim_{T\to\infty} \frac{1}{T} \int_{-T/2}^{T/2} dt \quad \hat{x}\hat{x}^{+} \tag{8.70}$$

[7] For the covariance, one can have two processes $Cov(\tau) = \langle (x(t+\tau) - \langle x \rangle)(y(t) - \langle y \rangle) \rangle$.

and therefore the spectrum can be expressed as

$$S(\omega) = \lim_{T\to\infty} \frac{1}{T} \int_{-T/2}^{T/2} e^{i\omega t} x(t) dt \quad \int_{-T/2}^{T/2} e^{-i\omega t'} x(t') dt' \quad . \tag{8.71}$$

The "total" integrated spectral density equals the variance of the series. Thus the spectral density within a particular interval of frequencies can be viewed as the amount of the variance explained by those frequencies. Mathematically, the spectral density is defined for both negative and positive frequencies. However, due to symmetry of the function $S(\omega)$ is quite often displayed for positive values only.

Let us calculate the inverse Fourier transformation of $S(\omega)$ and calculate the relation to the autocovariance function $Cov(\tau)$ of the stationary process $x(t)$:

$$\begin{aligned}
&\frac{1}{2\pi} \int_{\mathsf{R}} \; S(\omega) \;\; e^{-i\omega\tau} d\omega \\
&\qquad = \quad \lim_{T\to\infty} \frac{1}{T} \int_{\mathsf{R}} d\omega \frac{e^{-i\omega\tau}}{2\pi} \int_{-T/2}^{T/2} e^{i\omega t} x(t) dt \int_{-T/2}^{T/2} e^{-i\omega t'} x(t') dt' \\
&\qquad = \quad \lim_{T\to\infty} \frac{1}{T} \int_{-T/2}^{T/2} \int_{-T/2}^{T/2} \left(\frac{1}{2\pi} \int_{\mathsf{R}} e^{i\omega(t-t'-\tau)} d\omega \right) x(t) x(t') dt dt' \\
&\qquad = \quad \lim_{T\to\infty} \frac{1}{T} \int_{-T/2}^{T/2} \int_{-T/2}^{T/2} \delta(t-t'-\tau) x(t) x(t') dt dt' \qquad (8.72) \\
&\qquad = \quad \lim_{T\to\infty} \frac{1}{T} \int_{-T/2}^{T/2} x(t) x(t-\tau) dt \qquad (8.73) \\
&\qquad = \quad \langle x(t) x(t-\tau) \rangle \quad = \quad Cov(\tau) \qquad (8.74)
\end{aligned}$$

The transformation (8.72) comes from the Fourier transform of the $\delta-$function:

$$\int_{\mathsf{R}} e^{-i\omega t}\delta(t)dt = 1 \quad \longrightarrow \quad \delta(t) = \frac{1}{2\pi}\int_{\mathsf{R}} e^{i\omega t}d\omega \tag{8.75}$$

As the frequency domain counterpart of the autocovariance function of a stationary process, one can calculate the spectrum as

$$S(\omega) = \widehat{Cov(\tau)} \quad , \tag{8.76}$$

where the hat denotes again the Fourier transformation. This is the Wiener-Chinchin theorem, relating the sprectrum of a random process to its autocorrelation function (Fig. **??**).

The white noise process

The white noise process is therefore a function with constant $S(\omega)$, since the autocovariance is a delta dunction (8.67). The color of a noise signal (a signal produced by a stochastic process) is generally understood to be some broad characteristic of its power spectrum. This sense of 'color' for noise signals is similar to the concept of timbre in music (which is also called "tone color"); however the latter is almost always used for sound, and may consider very detailed features of the spectrum. The practice of naming kinds of noise after colors started with white noise, a signal whose spectrum has equal power within any equal interval of frequencies. That name was given by analogy with white light, which was (incorrectly) assumed to have such a flat power spectrum over the visible range. Other color names, like pink, red, and blue were then given to noise with other spectral profiles, often (but not always) in reference to the color of light with similar spectra. Some of those names have standard definitions in certain disciplines, while others are very informal and poorly defined. Noise is somehow opposite to music where we hear distinct frequencies (see for the frequencies of music: https://en.wikipedia.org/wiki/Piano_key_frequencies).

In equal temperament, one starts from a reference such as the note A, which is usually taken to

have frequency 440 Hz. All other notes have frequencies of the form 440 Hz $*a^n$ where n is the number of semitones between the note in question and the reference note A. The ratio of an equal-tempered semitone is $a = \sqrt[12]{2} = 1.05946$ $(a^{12} = 2)$. In equal temperament, enharmonic notes such as $C^{\#}$ and D^b are acoustically identical, they share the same frequency. Equal temperament was well-suited for the kind of music that was written from the eighteenth century onward, with its much greater range of modulations and chromatic harmonic vocabulary.

In Pythagorean tuning, intervals are derived by successions of perfect fifths, so the corresponding frequency ratios are powers of $3/2$. In conventional Western music, twelve perfect fifths in succession,

$$C - G - D - A - E - B - F^{\#} - C^{\#} - G^{\#} - D^{\#} - A^{\#} - E^{\#} - B^{\#},$$

are supposed to equal seven octaves (C = B#). However, since $(3/2)^{12}$ does not equal 2^7, twelve Pythagorean perfect fifths give an interval slightly larger than seven octaves. The difference is a small interval known as the Pythagorean comma, which corresponds to a ratio of $(3/2)^{12}$ to $2^7 \approx 1.013643$. The system of equal temperament gradually became adopted because it removed the limitations on keys for modulation. The discrepancies between just and equaltempered intervals are small and easily accepted by most listeners.

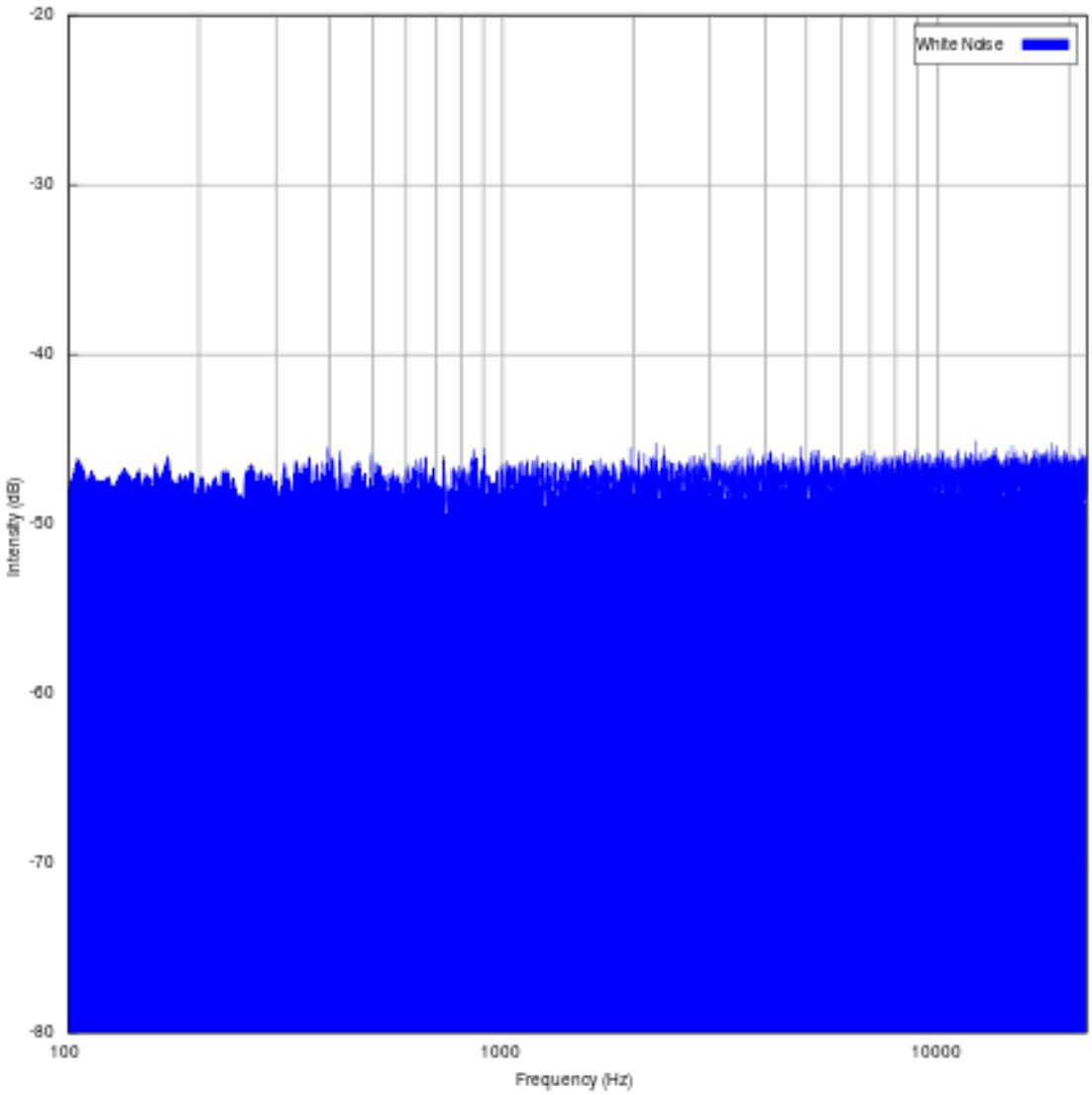

Figure 8.10: White noise spectrum. Flat power spectrum. (logarithmic frequency axis). For example, with a white noise audio signal, the range of frequencies between 40 Hz and 60 Hz contains the same amount of sound power as the range between 400 Hz and 420 Hz, since both intervals are 20 Hz wide. Note that spectra are often plotted with a logarithmic frequency axis rather than a linear one, in which case equal physical widths on the printed or displayed plot do not all have the same bandwidth, with the same physical width covering more Hz at higher frequencies than at lower frequencies. In this case a white noise spectrum that is equally sampled in the logarithm of frequency (i.e., equally sampled on the X axis) will slope upwards at higher frequencies rather than being flat.

8.4 Projection methods: coarse graining*

In order to get a first idea of coarse graining, one one may think of the transition from Rayleigh-Bénard convection to the Lorenz system (section 2.2). In our formula, the Galerkin approximation (2.40,2.40) provided a suitable projector to simply truncate the series at some specified wave number cut-off into a low-order system (such as in equations (2.41, 2.42).

The Mori-Zwanzig formalism [Mori, 1965; Zwanzig, 1960] provides a conceptual framework for the study of dimension reduction and the parametrisation of uninteresting variables by a stochastic process. It includes a generalized Langevin [1908] theory. Langevin [1908] studied Brownian motion from a different perspective to Einstein's seminal 1905 paper [Einstein, 1905], describing the motion of a single Brownian particle as a dynamic process via a stochastic differential equation, as an Ornstein-Uhlenbeck process [Uhlenbeck and Ornstein, 1930].

Ehrenfest introduced a special operation, the coarse-graining. This operation transforms a probability density in phase space into a "coarse-grained" density, that is a piecewise constant function, a result of density averaging in cells. The size of cells is assumed to be small, but finite, and does not tend to zero. The coarse-graining models uncontrollable impact of surrounding (of a thermostat, for example) onto ensemble of mechanical systems. To understand reasons for introduction of this new notion, let us take a phase drop, that is, an ensemble of mechanical systems with constant probability density localized in a small domain of phase space. Let us watch evolution of this drop in time according to the Liouville equation. After a long time, the shape of the drop may be very complicated, but the density value remains the same, and this drop remains "oil in water." The ensemble can tend to the equilibrium in the weak sense only: average value of any continuous function tends to its equilibrium value, but the entropy of the distribution remains constant. Nevertheless, if we divide the phase space into cells and supplement the mechanical motion by the periodical averaging in cells (this is the Ehrenfests' idea of coarse-graining), then the entropy increases, and the distribution density tends uniformly to the equilibrium. This periodical coarse-graining is illustrated by Fig. 8.11 in a two-dimensional phase space.

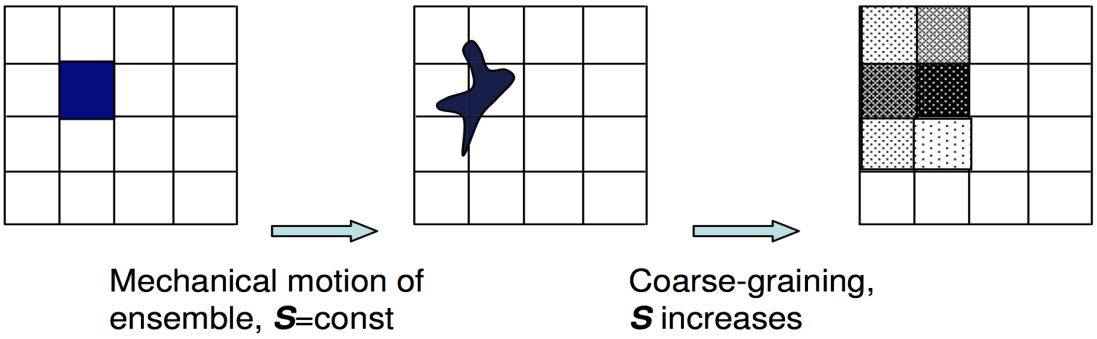

Figure 8.11: The Ehrenfests coarse-graining: two motion - coarse-graining cycles in 2D (values of probability density are presented by hatching density).

Applications of the Ehrenfests' coarse-graining[8] outside statistical physics include simple, but effective filtering. The Gaussian filtering of hydrodynamic equations that leads to the Smagorinsky equations[9] is, in its essence, again a version of the Ehrenfests' coarse-graining. The central idea of the Ehrenfests' coarse-graining remains the same in most generalizations: we combine the genuine motion with the periodic partial equlibration. The result is the Ehrenfests' chain. After that, we can find the macroscopic equation that does not depend on an initial distribution and describes the Ehrenfests' chains as results of continuous autonomous motion. Alternatively, we can just create a computational procedure without explicit equations. In the sense of entropy production, the resulting macroscopic motion is "more dissipative" than initial (microscopic) one. It is the theorem about entropy overproduction. In practice, kinetic models in the form of lattice Boltzmann models are in use (section9.2). The coarse-graining provides theoretical basis for kinetic models. First of all, it is possible to replace projecting (partial equilibration) by involution (i.e. reflection with respect to the partial equilibrium). This entropic involution was developed for the lattice Boltzmann methods. In the original Ehrenfests' chains, "motion-partial equilibration-motion-...," dissipation is coupled with time step, but the chains "motion-involution-motion-..." are conservative. The

[8] P. Ehrenfest, T. Ehrenfest-Afanasyeva, The Conceptual Foundations of the Statistical Approach in Mechanics, In: Mechanics Enziklopädie der Mathematischen Wissenschaften, Vol. 4., Leipzig, 1911. Reprinted: P. Ehrenfest, T. Ehrenfest-Afanasyeva, The Conceptual Foundations of the Statistical Approach in Mechanics, Dover Phoneix, 2002.

[9] J. Smagorinsky, General Circulation Experiments with the Primitive Equations: I. The Basic Equations, Mon. Weather Rev. 91 (1963), 99–164.

family of chains between conservative (with entropic involution) and maximally dissipative (with projection) ones give us a possibility to model hydrodynamic systems with various dissipation (viscosity) coefficients that are decoupled with time steps.

Of particular interest is the work of Mori [Mori, 1965] and Zwanzig [Zwanzig, 1960] which relates the evolution of macroscopic variables to microscopic dynamics. The standard Mori-Zwanzig theory has been given a nonlinear generalization by Zwanzig [Zwanzig, 1980], and is furthermore not limited to Hamiltonian dynamics [Chorin et al., 1999; Gottwald, 2010]. This approach of modelling fast small-scale processes by a stochastic process is intuitive: provided the fast processes decorrelate rapidly enough, the slow variables experience the sum of uncorrelated events of the fast dynamics, which according to the (weak) central limit theorem corresponds to approximate Gaussian noise. A method whereby many fast degrees of freedom are replaced by a stochastic process is called stochastic model reduction.

Consider the very simple coupled linear system[10]

$$\dot{\boldsymbol{x}} = \boldsymbol{L_{11}x} + \boldsymbol{L_{12}y} \qquad \text{the "climate" equation} \tag{8.77}$$

$$\dot{\boldsymbol{y}} = \boldsymbol{L_{21}x} + \boldsymbol{L_{22}y} \qquad \text{the "whether" equation.} \tag{8.78}$$

Suppose we are only interested in the dynamics of $\boldsymbol{x}$, and have only some climatic knowledge of the initial conditions of the variables y, that is the mean and variance. The whether differential equation (8.78) can be solved by the ansatz

$$\boldsymbol{y(t)} = \boldsymbol{e^{L_{22}t}y(0)} \cdot \boldsymbol{C(t)} \tag{8.79}$$

Inserting this, we can then solve the inhomogenous problem to obtain

$$\boldsymbol{y(t)} = \boldsymbol{e^{L_{22}t}y(0)} + \int_0^t \boldsymbol{e^{L_{22}(t-s)}L_{21}x(s)ds},$$

[10]We follow the notation of [Hasselmann, 1976; Chorin et al., 1999; Gottwald, 2010].

which we may use to express the dynamics of the climate variable as

$$\dot{\boldsymbol{x}} = \boldsymbol{L_{11}x} + \boldsymbol{L_{12}} \int_0^t \boldsymbol{e^{L_{22}(t-s)} L_{21} x(s) ds} + \boldsymbol{L_{12} e^{L_{22}t} y(0)}. \tag{8.80}$$

This is of the form of a generalised Langevin equation, where the first term is Markovian (no dependence on the history of the process), the second is a memory term, and the last can be interpreted as a noise term, provided that the initial conditions $\boldsymbol{y(0)}$ are randomly distributed. A similar reduction of the dynamics can be described by fast and slow variables applying the center manifold theory [Arnold, 1995] or slaving principle [Haken, 1996].

For the more general non-linear case, the instantaneous state of the Earth System, comprising the components 'atmosphere-ocean-cryosphere-land', can be expressed by a set of variables $\mathbf{z} = (z_1, z_2, ...)$, representing the density, velocity, temperature, etc. of the various media. The evolution of this system will be given by a series of prognostic equations of the form

$$\dot{\boldsymbol{z}} = \boldsymbol{f(z)}, \tag{8.81}$$

with initial condition $\boldsymbol{z(0)} = \boldsymbol{z_0}$ and $\boldsymbol{z} \in \boldsymbol{R^d}$, suppose we are not interested in the full solution $\boldsymbol{z(t)}$, but rather only in a few $\boldsymbol{n} \leq \boldsymbol{d}$ observables $\boldsymbol{\Phi(z)} = \boldsymbol{(\Phi_1(z), \Phi_2(z), ..., \Phi_n(z))}$. This includes the case $\boldsymbol{\Phi(z)} = \boldsymbol{(z_1, ..., z_n)}$, when the state space is decomposed as $\boldsymbol{z} = \boldsymbol{(x, y)}$ into 'interesting' variables, $\boldsymbol{x} = \boldsymbol{(z_1, ..., z_n)} \in \mathbb{R}^n$, and 'uninteresting' variables, $\boldsymbol{y} = \boldsymbol{(z_{n+1}, ..., z_d)} \in \mathbb{R}^{d-n}$. In the Earth System, a separation may be into a fast 'weather subsystem' (y) and a slow 'climate subsystem' (x) with different order of magnitude in the correlation times (or, the response/relaxation times) for the slow variable is much larger than that of the fast variable, i.e.

$$\boldsymbol{\tau_y \ll \tau_x}. \tag{8.82}$$

Now let us ask the following question: what are the effective dynamics of the interesting observables for an ensemble of initial conditions $\boldsymbol{z(0)}$, where $\boldsymbol{\Phi(z(0))}$ is known and the uninteresting subspace is equipped with a known distribution?

Rather than investigating the dynamical system (8.81) directly, one may choose to look at how observables $V(z(t))$ evolve in time. Applying the chain rule, one can naturally define the generator

$$\mathcal{L} = f(z) \cdot \nabla,$$

and write

$$\frac{d}{dt} V(z(t)) = \mathcal{L} V(z(t)).$$

Note that $\mathcal{L}$ is the adjoint operator of the Liouville operator $\mathcal{L}^*$ with $\mathcal{L}^* \rho = -\nabla \cdot (f(z)\rho)$ controlling the evolution of densities of ensembles propagated according to (8.81). We seek for the solution $v(z,t)$ of

$$\frac{\partial v}{\partial t} = \mathcal{L} v \text{ with } v(z,0) = \phi(z), \tag{8.83}$$

where z is an independent variable and denotes initial conditions. The solution of (8.83) can be formally written as

$$v(z,t) = e^{\mathcal{L}t} \phi(z), \tag{8.84}$$

To filter out the dynamics of the interesting variables we require a projection operator $\mathbf{P}$ that maps functions of $\mathbf{z}$ to functions of $\Phi(z)$. If the manifold consists for example of a product of submanifolds of relevant and irrelevant variables, one can take a conditional expectation

$$(\mathbf{P}v)(\mathbf{x}) = \frac{\int_{\mathbb{R}^{d-n}} v(z)\rho(\mathbf{x},\mathbf{y})d\mathbf{y}}{\int_{\mathbb{R}^{d-n}} \rho(\mathbf{x},\mathbf{y})d\mathbf{y}} \tag{8.85}$$

where $\rho(\mathbf{x},\mathbf{y})$ denotes the joint probability function of the initial conditions for the full system (8.81). It is easy to show that this a projection ($\mathbf{P^2} = \mathbf{P}$). In the context of PDEs one may use Galerkin approximations, a perfectly valid projector would be to simply truncate the Galerkin series at some specified high wave number cut-off. We also define the orthogonal projector $\mathbf{Q}$ that projects onto $\mathbf{y}$, with $\mathbf{Q} = \mathbf{1} - \mathbf{P}$. Now, the derivation of the Mori-Zwanzig equation is a two-linear: given the Cauchy problem (8.83) and its formal solution (8.84) we write, using

$\mathbf{P} + \mathbf{Q} = \mathbf{1}$,

$$\frac{\partial v}{\partial t}(z,t) = \mathcal{L}e^{\mathcal{L}t}\Phi(z) = e^{\mathcal{L}t}P\mathcal{L}\Phi(z) + e^{\mathcal{L}t}Q\mathcal{L}\Phi(z)$$

which, upon using the Duhamel-Dyson formula [Evans and Morriss, 2008] for operators A and B, yields

$$e^{t(A+B)} = e^{tA} + \int_0^t e^{(t-s)(A+B)}Be^{sA}ds.$$

By differentiation, this becomes the celebrated Mori-Zwanzig equation [Mori et al., 1974; Zwanzig, 1960]

$$\frac{\partial v}{\partial t}(z,t) = e^{\mathcal{L}t}P\mathcal{L}\Phi(z) + \int_0^t e^{(t-s)\mathcal{L}}P\mathcal{L}e^{sQ\mathcal{L}}Q\mathcal{L}\Phi(z)ds + e^{tQ\mathcal{L}}Q\mathcal{L}\Phi(z). \tag{8.86}$$

Note that the Mori-Zwanzig equation (8.86) is not an approximation but is exact and constitutes an equivalent formulation of the full problem (8.81). The Mori-Zwanzig equation (8.86) is in the form of a generalised Langevin equation. The first term on the right-hand side is Markovian, the second term is a memory term, and the last term lives in the uninteresting orthogonal subspace and can be called noise. Ideally one would like to approximate the noise term by white noise. Heuristically this should be possible in the case of time-scale separation or of weak coupling. The advantage of looking at this limit is however that the noise autocorrelation function and memory kernel can now be written as simple correlation and response functions of the unresolved dynamics. The reader is referred to [Chorin and Hald, 2006; Chorin et al., 2000; Zwanzig, 2001; Evans and Morriss, 2008; Givon et al., 2004; Lucarini et al., 2014] for more details.

The projection method includes the procedure to parameterize the turbulent energy dissipation in turbulent flows, where the larger eddies extract energy from the mean flow and ultimately transfer some of it to the smaller eddies which, in turn, pass the energy to even smaller eddies, and so on up to the smallest scales, where the eddies convert the kinetic energy into internal energy of the fluid. At this scales (also known as Kolmogorov scale), the viscous friction dominates the flow [Frisch, 1996].

The theory of scientific reduction is important for different theories: the microscopic informa-

tion in the brain with enormous amount of possible solutions is reduced to macroscopic actions and human behaviour. This implies that the actions are not deterministic, but stochastic in the sense of the standard Mori-Zwanzig theory or Brownian motion. Without being a specialist, this seems to be important for neuroscience and for the philosophy of science in general. The activity of neurons in the brain can be modelled statistically (e.g., https://en.wikipedia.org/wiki/Ising_model).

Chapter 9

Statistical Mechanics and Fluid Dynamics

The structure of fluid dynamical models is valid for systems with many degrees of freedom, many collisions, and for substances which can be described as a continuum. The transition from the highly complex dynamical equations to a reduced system is an important step since it gives more credibility to the approach and its results. The transition is also necessary since the active entangled processes are running on spatial scales from millimetres to thousands of kilometres, and temporal scales from seconds to millennia. Therefore, the unresolve processes on subgrid scales have to be described. This is the typical problem in statistical physics: How can we obtain the macroscopic dynamics from the underlying theory? Two different solutions are known, one is the so-called Mori-Zwanzig approach [Mori, 1965; Zwanzig, 1960, 1980] which relates the evolution of macroscopic variables to microscopic dynamics. The basic idea is the evolution of a system through a projection on a subset (macroscopic relevant part), where a randomness reflects the effects of the unresolved degrees of freedom. A particular example is the Brownian motion [Einstein, 1905; Langevin, 1908]. The other solution for the transition form the micro to macro-scales goes back to Boltzmann [1896]. The Boltzmann equation, also often known as the Boltzmann transport equation [Boltzmann, 1896; Bhatnagar et al., 1954; Cercignani, 1990] describes the statistical distribution of one particle in a fluid. It is one of the most important equations of non-equilibrium statistical mechanics, the area of statistical mechanics that deals with systems far from thermody-

namic equilibrium. It is applied, for instance, when there is an applied temperature gradient or electric field. Both, the Mori-Zwanzig and Boltzmann approaches play also a fundamental role in physics. The microscopic equations show no preferred time direction, whereas the macroscopic phenomena in the thermodynamics have a time direction through the enthropy. The underlying procedure is that part of the microscopic information is lost through coarse graining in space and time. Chapter 9 describes the approach from statistical mechanics towards the macroscopic theory. The Boltzmann equation and the Brownian motion are **the** approaches to understand the transition from micro to macro scales. For climate, this transition between the climate and weather scales has been formulated [Hasselmann, 1976; Leith, 1975], and later re-formulated in a mathematical context [Arnold, 2001; Chorin et al., 1999; Gottwald, 2010]. The effect of the weather on climate is seen by red-noise spectra in the climate system, showing one of the most fundamental aspects of climate, and serving also as a null hypothesis for climate variability studies. Chapter 9.4 deals with a fluid dynamical application, a 2D implementation of the Lattice Boltzmann Method (LBM) with the Bhatnagar-Gross-Krook (BGK) collision operator. The main structural parts of the program and several hints for the potential users are provided. While we do include a brief outline of the theory of LBM, detailed explanations are out of the scope of this book. Fore more details, please consult the references herein. The present code is intended to serve mainly as a showcase/practical introduction to Lattice Boltzmann Methods, hence advanced features and state-of-the-art algorithm improvements have been intentionally ommitted in favor of simplicity. One practical example, the Rayleigh-Benard convection [Rayleigh, 1916], is presented.

There are two ways of changing the descrition of the dynamics: from the micro to the macro scales. This is a common problem since we are not able to describe the systems on all temporal and spatial scales. One straitforward approach is coarse graining where the underlying dynamics is projected onto the macroscopic dynamics (section 8.4), the other is the statistical physics theory of non-equilibrium statistical mechanics (section 9.2).

A general question within the micro-macro dynamic is that of integration between the two different levels. Two distinctly different levels emerge with different rules governing each, but

they then need to be reconciled in some way to create an overall functioning system. Physical, chemical, biological, economic, social and cultural systems all exhibit this micro-macro dynamic and how the system comes to reconcile it forms a primary determinate in its identity and overall structure. This multi-dimensional nature to a system that results in the micro-macro dynamic is a product of synthesis and emergence. In many instances when we put elements together they do not simply remain discrete separate entities but they interact, co-evolve and they differentiate their states and function with respect to each other to become an interdependent whole, which comes to have properties and features that none of its parts possess. A whole new level of organization emerges that is different from the parts. This is made manifest in ecosystems; as they have co-evolved over millennia the parts are intricately interdependent forming a whole system that has features and dynamics independent from any of its parts and thus a two-tier system and a resulting emergent micro-macro dynamic. The whole ecosystem goes through processes of change - such as ecological succession - that are not associated with any of the parts but condition what creatures can viably exist within that macro regime.

We start from the point of view of kinetic theory of fluids where a gas is composed of a set of interacting particles Boltzmann [1896]. We are then interested in the probability of finding a fluid particle at a certain point in space and with a certain velocity. The moments of this probablility are related to our macroscopic fluid-dynamical quantities like density or velocity.

9.1 Mesoscopic dynamics*

Liouville equation

In the deterministic framework, the dynamics is characterized by

$$\frac{d}{dt}x(t) = f(x(t)) \quad , \tag{9.1}$$

and in the special case of classical mechanics can be descibed by a set of differential equations known as the Hamilton equations for that system. Hamiltonians can be used to describe such simple systems as a bouncing ball, a pendulum or an oscillating spring in which energy changes from kinetic to potential and back again over time. Hamiltonians can also be employed to model the energy of other more complex dynamic systems such as planetary orbits in celestial mechanics and also in quantum mechanics. The Hamilton equations are generally written as follows:

$$\dot{\boldsymbol{p}} = -\frac{\partial \mathcal{H}}{\partial \boldsymbol{q}} \tag{9.2}$$

$$\dot{\boldsymbol{q}} = \frac{\partial \mathcal{H}}{\partial \boldsymbol{p}} \tag{9.3}$$

In the above equations, the dot denotes the ordinary derivative with respect to time of the functions $\boldsymbol{p} = \boldsymbol{p}(t)$ (called generalized momenta) and $\boldsymbol{q} = \boldsymbol{q}(t)$ (called generalized coordinates), taking values in some vector space, and $\mathcal{H} = \mathcal{H}(\boldsymbol{p}, \boldsymbol{q}, t)$ is the so-called Hamiltonian, or (scalar valued) Hamiltonian function. The associated probability distribution for the generalized dynamics (9.1) is given in the phase space

$$\boldsymbol{p}(\boldsymbol{x}, t) = \delta(\boldsymbol{x} - \boldsymbol{x}(t)) \tag{9.4}$$

yielding the Liouville equation

$$\partial_t \boldsymbol{p} = -\frac{\boldsymbol{d}}{\boldsymbol{dx}(\boldsymbol{t})} \left[\delta(\boldsymbol{x} - \boldsymbol{x}(t))\right] \frac{\boldsymbol{d}}{\boldsymbol{dt}} \boldsymbol{x}(t) = -\frac{\partial \boldsymbol{p}}{\partial \boldsymbol{x}} \boldsymbol{f}(\boldsymbol{x}) \quad . \tag{9.5}$$

The Liouville equation is often used in the framework of the Hamiltonian dynamics (9.3). Since the phase space velocity $(\dot{\boldsymbol{p}}_i, \dot{\boldsymbol{q}}_i)$ has zero divergence, and probability is conserved. Its substantial derivative can be shown to be zero and so

$$\frac{\partial}{\partial t} \rho = -\{\, \rho, \mathcal{H} \,\}. \tag{9.6}$$

using the Poisson bracket

$$\{f, g\} = \sum_{i=1}^{N} \left[\frac{\partial f}{\partial q_i} \frac{\partial g}{\partial p_i} - \frac{\partial f}{\partial p_i} \frac{\partial g}{\partial q_i} \right]. \tag{9.7}$$

Master equation

The master equation is a phenomenological set of first-order differential equations describing the time evolution of the probability of a system to occupy each one of a discrete set of states:

$$\frac{dP_k}{dt} = \sum_{\ell} T_{k\ell} P_{\ell}, \tag{9.8}$$

where P_k is the probability for the system to be in the state k, while the matrix $T_{\ell k}$ is filled with a grid of transition-rate constants. In probability theory, this identifies the evolution as a continuous-time Markov process, with the integrated master equation obeying a Chapman-Kolmogorov equation. Note that

$$\sum_{\ell} T_{\ell k} = 0 \tag{9.9}$$

(i.e. probability is conserved), so the equation may also be written as

$$\frac{dP_k}{dt} = \sum_{\ell} (T_{k\ell} P_{\ell} - T_{\ell k} P_k). \tag{9.10}$$

allowing us to omit the term $\ell = k$ from the summation. Thus, in the latter form of the master equation there is no need to define the diagonal elements of T.

The master equation exhibits detailed balance if each of the terms of the summation disappears separately at equilibrium, i.e. if, for all states k and l having equilibrium probabilities pi_k and π_{ℓ}

$$T_{k\ell} \pi_{\ell} = T_{\ell k} \pi_k \tag{9.11}$$

Many physical problems in classical, quantum mechanics and problems in other sciences, can be reduced to the form of a master equation, thereby performing a great simplification of the problem. In the continous case, the Chapman-Kolmogorov equation has similarities with the Master equation. The Chapman-Kolmogorov equation is an identity relating the joint probability distributions of different sets of coordinates on a stochastic process. Suppose that $\{x_i\}$ is an indexed collection of random variables, that is, a stochastic process. Let

$$p_{i_1,\ldots,i_n}(x_1,\ldots,x_n) \tag{9.12}$$

be the joint probability density function of the values of the random variables $x1$ to x_n. Then, the Chapman-Kolmogorov equation is

$$p_{i_1,\ldots,i_{n-1}}(x_1,\ldots,x_{n-1}) = \int_{-\infty}^{\infty} p_{i_1,\ldots,i_n}(x_1,\ldots,x_n)\, dx_n \tag{9.13}$$

i.e. a straightforward marginalization over the nuisance variable.

When the stochastic process under consideration is Markovian, the Chapman-Kolmogorov equation is equivalent to an identity on transition densities. In the Markov chain setting, one assumes that $i_1 < \ldots < i_n$. Then, because of the Markov property,

$$p_{i_1,\ldots,i_n}(x_1,\ldots,x_n) = p_{i_1}(x_1)p_{i_2;i_1}(x_2 \mid x_1)\cdots p_{i_n;i_{n-1}}(x_n \mid x_{n-1}), \tag{9.14}$$

where the conditional probability $p_{i;j}(x_i \mid x_j)$ is the transition probability between the times $i > j$. So, the Chapman-Kolmogorov equation takes the form

$$p_{i_3;i_1}(x_3 \mid x_1) = \int_{-\infty}^{\infty} p_{i_3;i_2}(x_3 \mid x_2)p_{i_2;i_1}(x_2 \mid f_1)\, dx_2. \tag{9.15}$$

When the probability distribution on the state space of a Markov chain is discrete and the Markov chain is homogeneous, the Chapman-Kolmogorov equations can be expressed in terms of (possibly

infinite-dimensional) matrix multiplication, thus:

$$\boldsymbol{P}(t+s) = \boldsymbol{P}(t)\boldsymbol{P}(s) \tag{9.16}$$

where P(t) is the transition matrix, i.e., if Xt is the state of the process at time t, then for any two points i and j in the state space, we have

$$\boldsymbol{P}_{ij}(t) = \boldsymbol{P}(\boldsymbol{X}_t = j \mid \boldsymbol{X}_0 = i). \tag{9.17}$$

Example for the Chapman-Kolmogorov and Master equations in climate dynamics are related to transitions between different states.

Fokker-Planck dynamics

In the stochastic context, we make a Taylor expansion up to order two in $\boldsymbol{dx} = \boldsymbol{x}(\boldsymbol{t}+\boldsymbol{dt}) - \boldsymbol{x}(\boldsymbol{t})$ from the Master equation:

$$\begin{aligned}
\boldsymbol{dp} &= \boldsymbol{p}(\boldsymbol{x}, \boldsymbol{t}+\boldsymbol{dt}) - \boldsymbol{p}(\boldsymbol{x}, \boldsymbol{t}) \\
&= < \boldsymbol{\delta}(\boldsymbol{x} - \boldsymbol{x}(\boldsymbol{t}+\boldsymbol{dt})) > - < \boldsymbol{\delta}(\boldsymbol{x} - \boldsymbol{x}(\boldsymbol{t})) > \\
&= - < \frac{\boldsymbol{d}}{\boldsymbol{dx}(\boldsymbol{t})} \left[\boldsymbol{\delta}(\boldsymbol{x} - \boldsymbol{x}(\boldsymbol{t}))\right] \, \boldsymbol{dx} > + \frac{\mathbf{1}}{\mathbf{2}} < \frac{\boldsymbol{d^2}}{\boldsymbol{dx^2}} \left[\boldsymbol{\delta}(\boldsymbol{x} - \boldsymbol{x}(\boldsymbol{t}))\right] \, \boldsymbol{dx^2} > \\
&= - \frac{\boldsymbol{\partial p}}{\boldsymbol{\partial x}} < \boldsymbol{dx} > + \frac{\mathbf{1}}{\mathbf{2}} \frac{\boldsymbol{\partial^2}}{\boldsymbol{\partial x^2}} \boldsymbol{p} \, < \boldsymbol{dx^2} > \\
&= - \frac{\boldsymbol{\partial p}}{\boldsymbol{\partial x}} \boldsymbol{f}(\boldsymbol{x}) \boldsymbol{dt} + \frac{\mathbf{1}}{\mathbf{2}} \frac{\boldsymbol{\partial^2}}{\boldsymbol{\partial x^2}} \boldsymbol{p} \, \boldsymbol{g^2 dt}
\end{aligned} \tag{9.18}$$

The probability density $\boldsymbol{p}(\boldsymbol{x}, \boldsymbol{t})$ for the variable $\boldsymbol{x}(\boldsymbol{t})$ in (8.8) obeys therefore the Fokker-Planck equation

$$\boldsymbol{\partial_t p} = - \frac{\boldsymbol{\partial}}{\boldsymbol{\partial x}} \left[\boldsymbol{f}(\boldsymbol{x}) \boldsymbol{p}\right] + \frac{\boldsymbol{\partial}}{\boldsymbol{\partial x}} \left[\boldsymbol{g}(\boldsymbol{x}) \frac{\boldsymbol{\partial}}{\boldsymbol{\partial x}} \left\{\boldsymbol{g}(\boldsymbol{x}) \boldsymbol{p}\right\}\right] \quad . \tag{9.19}$$

Its stationary probability density of (8.8) is given by

$$p_{st}(x) = \aleph \exp\left(-2\int_{x_0}^{x} \frac{f(y) - g(y)g'(y)}{g(y)^2}\, dy\right) \quad . \tag{9.20}$$

where $\aleph$ is a normalization constant. $g'(y)$ stands for the derivative of g with respect to its argument. The extrema x_m of the steady state density obey the equation

$$f(x_m) - g(x_m)g'(x_m) = 0 \tag{9.21}$$

for $g(x_m)n_e0$. Here is the crux of the noise-induced transition phenomenon: one notes that this equation is not the same as the equation $f(x_m) = 0$ that determines the steady states of the system in the absence of multiplicative noise. As a result, the most probable states of the noisy system need not to coincide with the deterministic stationary states. More importantly, new solutions may appear or existing solutions may be destabilized by the noise. These are the changes in the asymptotic behavior of the system caused by the presence of the noise, e.g. **?**.

9.2 The Boltzmann Equation*

One of the most significant theoretical breakthroughs in statistical physics was due to Ludwig Boltzmann (Boltzmann [1896], Boltzmann [1995] for a recent reprint of his famous lectures on kinetic theory), who pioneered non-equilibrium statistical mechanics. Boltzmann postulated that a gas was composed of a set of interacting particles, whose dynamics could be (at least in principle) modelled by classical dynamics. Due to the very large number of particles in such a system, a statistical approach was adopted, based on simplified physics composed of particle streaming in space and billiard-like inter-particle collisions (which are assumed elastic). Instrumental to the theory is the single-particle distribution function (hereafter SPDF), $f(\vec{x}, \vec{e}, t)$ which represents the probability density of having a particle at the point $(\vec{x}, \vec{e})$ in the phase space. Hence, the

quantity

$$f(\vec{x},\vec{e},t)d\vec{x}d\vec{e} \tag{9.22}$$

represents the probability of finding a particle inside an infinitesimal space cubelet centered around $\vec{x}$, and inside an infinitesimal momentum-space cubelet around $\vec{e}$ at any given time t. In the presence of a body-force $\vec{F}$, the SPDF will evolve according to

$$f(\vec{x}+d\vec{x},\vec{e}+d\vec{e},t+dt)d\vec{x}d\vec{e} = f(\vec{x},\vec{e},t)d\vec{x}d\vec{e}\,, \tag{9.23}$$

where $d\vec{x} = \vec{e}dt$ and $d\vec{e} = \vec{F}dt/m$. If we also include the effect of the collisions, and denote by $\Gamma_+ d\vec{x}d\vec{e}dt$ the probability for a particle to start from outside the $d\vec{x}\times d\vec{e}$ domain and to enter this phase-space region during the infinitesimal time dt and by $\Gamma_- d\vec{x}d\vec{e}dt$ the probability for a particle to start from the $d\vec{x}\times d\vec{e}$ domain and leave this phase-space region during the infinitesimal time dt, the evolution of the SPDF becomes

$$f(\vec{x}+d\vec{x},\vec{e}+d\vec{e},t+dt)d\vec{x}d\vec{e} = f(\vec{x},\vec{e},t)d\vec{x}d\vec{e} + (\Gamma_+ - \Gamma_-)\,d\vec{x}d\vec{e}dt \tag{9.24}$$

Expanding the LHS into a Taylor series around the phase-space point $(\vec{x},\vec{u},t)$, we obtain:

$$f(\vec{x}+d\vec{x},\vec{e}+d\vec{e},t+dt)d\vec{x}d\vec{e} = f(\vec{x},\vec{e},t)d\vec{x}d\vec{e} + \left(\frac{\partial f}{\partial t}\right)dt + (\nabla_{\vec{x}}f)\cdot d\vec{x} + (\nabla_{\vec{e}}f)\cdot d\vec{e} + \ldots \tag{9.25}$$

Inserting Eq. (9.25) into Eq. (9.24) and cancelling terms, we easily obtain Boltzmann's Equation:

$$\frac{\partial f}{\partial t} + \vec{e}\cdot\nabla_{\vec{x}}f + \vec{F}/m\cdot\nabla_{\vec{e}}f = \Gamma_+ - \Gamma_- \tag{9.26}$$

where $\nabla_{\vec{x}}$ is the gradient operator in physical space and $\nabla_{\vec{e}}$ the same in momentum space.[1]

For the sake of clarity, we have not written the collision operator explicitly yet. The important

[1]The collisionless Boltzmann equation is often mistakenly called the Liouville equation (the Liouville Equation is an N-particle equation being N the number of microscopic particles). The Boltzmann equation is a mesoscopic dynamics with degrees of freedom $<< N$.

point is that the separation of the dynamics into collisions and streaming is already apparent from Eq. (9.26). The collision operator, which is in itself a complex integro-differential expression, reads

$$\Gamma_+ - \Gamma_- \equiv \int d\vec{e}_1 \int d\Omega\, \sigma(\Omega)\, |\vec{e} - \vec{e}_1| \, \left[f(\vec{e}') f(\vec{e}_1') - f(\vec{e}) f(\vec{e}_1) \right] \tag{9.27}$$

where σ is the differential cross-section in the case of the 2-particle collisions (which is a function of the solid angle Ω only), unprimed velocities are incoming (before collision) and primed velocities are outgoing (after collision).[2] In another notation

$$\Gamma_+(\vec{x}, \vec{e}, t) = \int d\vec{e}_1 \int d\vec{e}' \int d\vec{e}_1' \quad P_{(e',e_1')\to(e,e_1)} \quad f(\vec{e}') f(\vec{e}_1') \tag{9.28}$$

$$\Gamma_-(\vec{x}, \vec{e}, t) = \int d\vec{e}_1 \int d\vec{e}' \int d\vec{e}_1' \quad P_{(e,e_1)\to(e',e_1')} \quad f(\vec{e}) f(\vec{e}_1) \tag{9.29}$$

where $P_{(e',e_1')\to(e,e_1)}$ is the probability density to go from initial state (e', e_1') to final state (e, e_1) in time dt. It follows from symmetry considerations that $P_{(e',e_1')\to(e,e_1)} = P_{(e,e_1)\to(e',e_1')}$ and

$$d\vec{e}' d\vec{e}_1' P_{(e',e_1')\to(e,e_1)} = d\Omega\, \sigma(\Omega)\, |\vec{e} - \vec{e}_1| \tag{9.30}$$

A fundamental property of the collision operator [Cercignani, 1987] is that it conserves mass, momentum and kinetic energy (hence also a linear combination thereof). Also, it can be shown that the local Maxwell-Boltzmann distribution pertains to a certain class of positive SPDFs for which the collision integral vanishes (variational principle, Lagrange parameters). It can be shown

[2] Of course, finding or modeling the collision term is the biggest challenge in the kinetic theory. In the simplest model one only takes into account binary collisions and assumes that the colliding particles are uncorrelated (i.e. molecular chaos assumption). The collisions are proportianal to the velocity difference between the particles $|\vec{u} - \vec{u}_1|$. Consider an elastic collision of two spherically symmetric (spin-less) molecules with mass m and velocities $\vec{e}$ and $\vec{e}_1$. After collision their respective velocities are $\vec{e}'$ and $\vec{e}_1'$. Then the following conservation laws apply:
Momentum conservation: $m(\vec{e} + \vec{e}_1) = m(\vec{e}' + \vec{e}_1')$.
Energy conservation: $m/2 \quad \vec{e} \cdot \vec{e} + m_1/2 \quad \vec{e}_1 \cdot \vec{e}_1 = m/2 \quad \vec{e}' \cdot \vec{e}' + m_1/2 \quad \vec{e}_1' \cdot \vec{e}_1' \quad .$

that this equilibrium distribution is given by

$$f_0(\vec{x},\vec{e}) = \rho(\vec{x})\left[\frac{m}{2\pi kT(\vec{x})}\right]^{3/2} \exp\{-m\left[\vec{e}-\vec{u}(\vec{x})\right]^2/2kT(\vec{x})\} \tag{9.31}$$

where $\rho(\vec{x}), \vec{u}(\vec{x})$ and $T(\vec{x})$ are the local density, macroscopic velocity, and temperature, respectively.[3] If there are no external forces such as gravity or electrostatic interactions we have $\rho(\vec{x}) = \rho_0 = N/V$. In case the temperature is also independent of position, and if the gas as a whole is not moving ($\vec{u} = 0$), then $f(\vec{x},\vec{e}) = \rho_0 f_0(\vec{e})$, with

$$f_0(\vec{e}) = \left[\frac{m}{2\pi kT}\right]^{3/2} e^{-m\vec{e}^2/2kT},$$

This implies that, if this distribution is attained, we also have a state where incoming SPDFs exactly balance the outgoing ones, maintaining a local dynamic equilibrium. This observation is of paramount importance for our method, which uses the (discretized) Maxwell-Boltzmann distribution as the equilibrium distribution functions.

9.3 H-Theorem and approximation of the Boltzmann equation*

The other important feature of this equation is that the integral

$$H = \int\int d\vec{x}d\vec{e}\; f(\vec{x},\vec{e},t)\ln f(\vec{x},\vec{e},t) \tag{9.34}$$

[3] This experssion of the SPDF can be approximated through a Taylor series of the exponential: $\exp(y) = 1 + y$. Task: Show that

$$f_a^{eq}(\vec{x},\vec{e}) = \rho(\vec{x})\left[1 + 3\frac{\vec{u}\cdot\vec{e}}{c_s^2} + \frac{9}{2}\frac{(\vec{u}\cdot\vec{e})^2}{c_s^4} - \frac{3}{2}\frac{\vec{e}^2}{c_s^2}\right], \tag{9.32}$$

with the speed of sound c_s and

$$\frac{1}{c_s^2} = \frac{1}{\gamma}\frac{m}{kT} \tag{9.33}$$

and γ the adiabatic factor.

can only decrease. This can be seen by using the following:

$$\frac{dH}{dt} = \int d\vec{e}_1 \int d\Omega\, \sigma(\Omega)\, |\vec{e} - \vec{e}_1|\, \left[f(\vec{e}')f(\vec{e}_1') - f(\vec{e})f(\vec{e}_1)\right] \left[1 + \ln f(\vec{e}_1)\right] \quad (9.35)$$

and the same term for

$$\frac{dH}{dt} = \int d\vec{e}_1 \int d\Omega\, \sigma(\Omega)\, |\vec{e} - \vec{e}_1|\, \left[f(\vec{e}')f(\vec{e}_1') - f(\vec{e})f(\vec{e}_1)\right] \left[1 + \ln f(\vec{e}_1')\right] \quad (9.36)$$

The term is also invariant with respect to the notation (’), i.e.

$$\frac{dH}{dt} = \int d\vec{e}_1 \int d\Omega\, \sigma(\Omega)\, |\vec{e} - \vec{e}_1|\, \left[f(\vec{e})f(\vec{e}_1) - f(\vec{e}')f(\vec{e}_1')\right] \left[1 + \ln f(\vec{e}_1')\right] \quad (9.37)$$

and

$$\frac{dH}{dt} = \int d\vec{e}_1 \int d\Omega\, \sigma(\Omega)\, |\vec{e} - \vec{e}_1|\, \left[f(\vec{e})f(\vec{e}_1) - f(\vec{e}')f(\vec{e}_1')\right] \left[1 + \ln f(\vec{e}_2')\right] \quad (9.38)$$

Use furthermore

$$\eta' = f(\vec{e}')f(\vec{e}_1') \quad \text{and} \quad \eta = f(\vec{e})f(\vec{e}_1) \quad (9.39)$$

$$E = (\eta' - \eta)\left[\ln \eta - \ln \eta'\right] \quad (9.40)$$

and recognize that E is negative. $\frac{d}{dt}H$ is equal zero for

$$f(\vec{e}')f(\vec{e}_1') = f(\vec{e})f(\vec{e}_1) \quad . \quad (9.41)$$

For a system of N statistically independent particles, H is related to the thermodynamic entropy S through:

$$S \stackrel{\text{def}}{=} -NkH \quad (9.42)$$

Therefore, according to the H-theorem, S can only increase.[4] The same function $\boldsymbol{H}$ is also used as "information function":

$$\boldsymbol{I} = -\sum_i \boldsymbol{f_i} \ln \boldsymbol{f_i} = < -\ln \boldsymbol{f} > . \tag{9.43}$$

where the $\boldsymbol{f_i}$ can be interpreted as probablity and not only as a measure of the breadth of the spread of states available to a single particle in a gas of like particles, where $\boldsymbol{f_i}$ represented the relative frequency distribution of each possible state. When all the probabilities $\boldsymbol{f_i}$ are equal, I is maximal, and we have minimal information about the system. When our information is maximal (i.e., one $\boldsymbol{f_i}$ is equal to one and the rest to zero, such that we know what state the system is in), the function is minimal. This information function is also called "reduced entropic function" in thermodynamics [Shannon, 1948]. Gibbs proposed a general formula for statistical-mechanical entropy, no longer requiring identical and non-interacting particles, but instead based on the probability distribution $\boldsymbol{p_i}$ for the complete microstate i of the total system:

$$\boldsymbol{S} = -\boldsymbol{k} \sum_i \boldsymbol{p_i} \ln \boldsymbol{p_i} \tag{9.44}$$

$$\frac{\boldsymbol{dS}}{\boldsymbol{dt}} = -\boldsymbol{k} \sum_i \left(\frac{\boldsymbol{dp_i}}{\boldsymbol{dt}} \ln \boldsymbol{p_i} + \frac{\boldsymbol{dp_i}}{\boldsymbol{dt}} \right) = -\boldsymbol{k} \sum_i \frac{\boldsymbol{dp_i}}{\boldsymbol{dt}} \ln \boldsymbol{p_i} \tag{9.45}$$

[4] Please see the link to the Lyapunov function for the Lorenz system in Chapter 2.2.

because $\sum_i \frac{dp_i}{dt} = \frac{d}{dt}\sum_i p_i = \frac{d}{dt}(1) = 0$. Now, formulate a master equation [van Kampen, 1981] for the average rate of jumps[5] from state α to β, and from state β to α:

$$\frac{dp_\alpha}{dt} = \sum_\beta \nu_{\alpha\beta}(p_\beta - p_\alpha) \tag{9.46}$$

$$\frac{dp_\beta}{dt} = \sum_\alpha \nu_{\alpha\beta}(p_\alpha - p_\beta) \tag{9.47}$$

where the reversibility of the dynamics ensures that the same transition constant $\nu_{\alpha\beta}$ appears in both expressions. So

$$\frac{dS}{dt} = \frac{1}{2}k\sum_{\alpha,\beta}\nu_{\alpha\beta}(\ln p_\beta - \ln p_\alpha)(p_\beta - p_\alpha). \tag{9.48}$$

But the two brackets will have the same sign (the same argument as in equation 9.40), so each contribution to dS/dt cannot be negative and therefore, $\frac{dS}{dt} \geq 0$ for an isolated system. Due to the complex expression for the collision operator, it became clear that approximations were desirable. It was also proven (see Cercignani [1990]) that such approximations were also reasonable, since the details of the two-body interaction are not likely to influence significantly experimentally-measured quantities. Hence, approximate collision operators were proposed, all of which had to $\boxed{1}$ conserve local mass, momentum and energy and $\boxed{2}$ develop a collisional contribution in Boltzmann's equation (9.26) which tends to a local Maxwellian distribution. It was soon realized that a model developed at the middle of last century Bhatnagar et al. [1954] (also known as Bhatnagar-Gross-Krook; hereafter BGK) satisfied both of these conditions. Chapman and Enskog developed a general procedure for the approximate solution of Boltzmann's equation. For certain simple model systems such as hard spheres their method produces predictions for (or its moments) which may

[5]The master equation is quite often written as: $\frac{d\vec{P}}{dt} = \mathbf{A}\vec{P}$, where $\vec{P}$is a column vector (where element i represents state i), and $\mathbf{A}$ is the matrix of connections. The way connections among states are made determines the dimension of the problem. When the connections are time-independent rate constants, the master equation represents a kinetic scheme and the process is Markovian (any jumping time probability density function for state i is an exponential, with a rate equal to the value of the connection). When the connections depend on the actual time (i.e. matrix $\mathbf{A}$ depends on the time, $\mathbf{A} \to \mathbf{A}(t)$), and the process is not stationary. For an application in meteorogy, e.g. Egger [2001].

be tested in computer simulations. Another more modern approach to the numerical solution of the transport equation is the "Lattice Boltzmann" method in which the continuous variables and are restricted to a set of discrete values; the time change of these values is then described by a modified transport equation which lends itself to fast computation. The moments of the distribution function represent macroscopic variables density and velocity fields:

$$\rho(\vec{x},t) = m\int d\vec{e} f(\vec{x},\vec{e},t) \tag{9.49}$$

$$\rho(\vec{x},t)\vec{u}(\vec{x},t) = m\int d\vec{e}\,\vec{e} f(\vec{x},\vec{e},t) \tag{9.50}$$

Note that the molecular velocities $\vec{e}$ is different from the macroscopic veleocity field $\vec{u}(\vec{x},t)$. The basic idea was that each collision changes the SPDF by an amount which is proportional to the departure from the local Maxwellian distribution:

$$\Gamma_+ - \Gamma_- = -\frac{f(\vec{x},\vec{e},t) - f_0(\vec{x},\vec{e})}{\tau} \tag{9.51}$$

with relaxation constant τ. In dimensionless units, τ is replaced by the dimensionless Knudsen number $Kn = l/L$ with l is the mean-free-path. It is the small parameter in the kinetics - fluid dynamics transition. If the $Kn >> 1$ then the continuum assumption of fluid mechanics is no longer a good approximation and kinetic equations must be used.

9.4 Application: Lattice Boltzmann Dynamics

9.4.1 Lattice Boltzmann Methods*

LBMs recently proved to be viable alternatives to traditional computational fluid dynamics (CFD). The latter adopts a strategy consisting of: writing the macroscopic flow equations; discretizing the macroscopic equations using finite differences, finite volumes or finite elements; solving the discretized equations on a computer. In contrast, LBM takes a different route towards the same results. The LBM approach is composed of formulating a mesoscopic model for the evolution of the PDF such that the desired macroscopic flow equations are obtained. The end result of both approaches are similar. However, the algorithms differ due to the different perspective on the physics of the flow. There are in principle an infinite set of possible mesoscopic models. However, we focus on the most common ones, which consist of a streaming and a collision process. These LBMs use a simplified collision operator Bhatnagar et al. [1954], hence they are also referred to as LBM-BGK models.

There are several possible choices for the underlying lattice. These are usually classified in the literature using the $\boldsymbol{D\alpha Q\beta}$-notation, where $\boldsymbol{\alpha}$ is an integer number denoting the space dimensionality and $\boldsymbol{\beta}$ is another integer indicating the number of discrete velocities (including the particle at rest) within the momentum discretization. Some restrictions have to be fulfilled (especially Galilean and rotational invariance)[6] to ensure that a particular discretization can simulate the Navier-Stokes equations. Among the lattices in common use there are the $\boldsymbol{D2Q9}$ and $\boldsymbol{D3Q19}$-models (see for example discussion in He and Luo [1997]). Our focus here is the $\mathbf{2}\boldsymbol{D}$ case, hence we have chosen the $\boldsymbol{D2Q9}$ momentum discretization. The discrete velocity directions for the $\boldsymbol{D2Q9}$ lattice are shown in Fig 9.1. The macroscopic variables are defined as functions of the

[6] A lattice with reduced symmetry can be (and has been) used, see d'Humieres et al. [2001], where a $\boldsymbol{D3Q13}$-lattice is used. However, this approach also departs from the classical BGK-LBM dynamics.

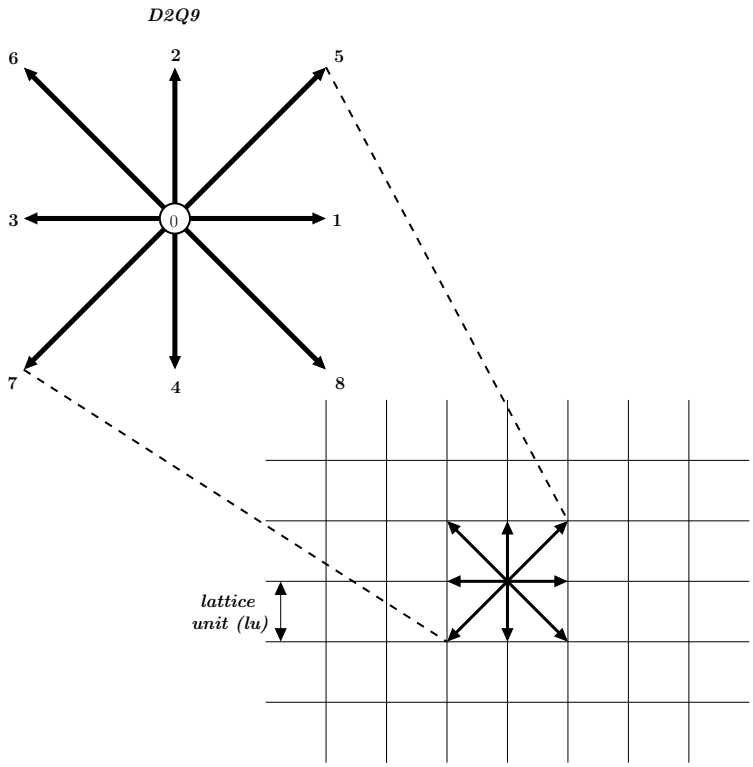

Figure 9.1: Discrete lattice velocities for the $\boldsymbol{D2Q9}$ model.

particle distribution functions (hereafter DFs) according to:

$$\boldsymbol{\rho} = \sum_{a=0}^{\beta-1} \boldsymbol{f_a} \qquad \text{(macroscopic fluid density)} \tag{9.52}$$

$$\text{and} \qquad \vec{\boldsymbol{u}} = \frac{1}{\boldsymbol{\rho}} \sum_{a=0}^{\beta-1} \boldsymbol{f_a} \vec{\boldsymbol{e}}_{\boldsymbol{a}} \qquad \text{(macroscopic velocity).} \tag{9.53}$$

The DFs at each lattice point are updated using the equation:

$$\underbrace{\boldsymbol{f_a}(\vec{\boldsymbol{x}} + \vec{\boldsymbol{e}}_{\boldsymbol{a}}\boldsymbol{\delta_t}, \boldsymbol{t} + \boldsymbol{\delta_t}) = \boldsymbol{f_a}(\vec{\boldsymbol{x}}, \boldsymbol{t})}_{\text{Streaming}} - \underbrace{\frac{[\boldsymbol{f_a}(\vec{\boldsymbol{x}}, \boldsymbol{t}) - \boldsymbol{f_a^{eq}}(\vec{\boldsymbol{x}}, \boldsymbol{t})]}{\boldsymbol{\tau}}}_{\text{Collision}}, \tag{9.54}$$

where $\boldsymbol{a} \in [\boldsymbol{0}, \boldsymbol{\beta - 1}]$ is an index spanning the (discretized) momentum space and $\boldsymbol{\tau}$ is a relaxation parameter, which is related to the fluid viscosity. The streaming step, where the DFs are translated

to the neighbouring sites according to the respective discrete velocity direction, is illustrated in Fig. 9.2, in the $\boldsymbol{D2Q9}$ model. The collision step (illustrated in Fig. 9.3) consists of a re-distribution of the DFs towards the local discretized Maxwellian equilibrium DFs, in such a way that local mass and momentum are invariant. The equilibrium DFs can be obtained from the local Maxwell-

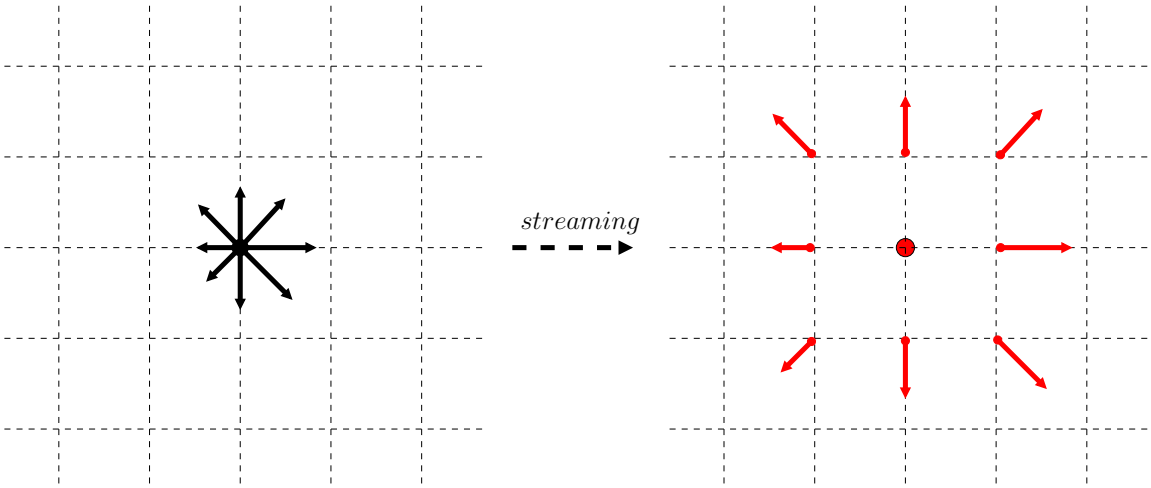

Figure 9.2: Illustration of the streaming process on a $\boldsymbol{D2Q9}$ lattice. Note that the magnitude of the DFs remain unchanged, but they move to a neighbouring node according to their direction.

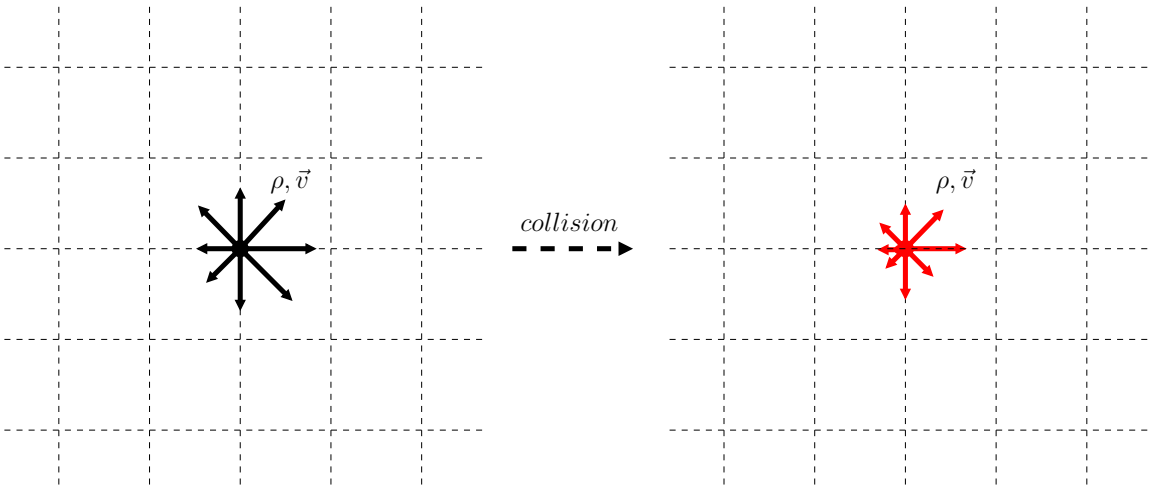

Figure 9.3: Illustration of the collision process on a $\boldsymbol{D2Q9}$ lattice. Note that the local density $\boldsymbol{\rho}$ and velocity $\vec{\boldsymbol{v}}$ are conserved, but the DFs change according to the relaxation-to-local-Maxwellian rule.

Boltzmann SPDF (see for example He and Luo [1997]); they are

$$f_a^{eq}(\vec{x}) = w_a \rho(\vec{x}) \left[1 + 3\frac{\vec{e}_a \cdot \vec{u}}{c^2} + \frac{9}{2}\frac{(\vec{e}_a \cdot \vec{u})^2}{c^4} - \frac{3}{2}\frac{\vec{u}^2}{c^2} \right], \tag{9.55}$$

where for the $D2Q9$ model the weights are $w_{a=0} = 4/9, w_{a=\{1..4\}} = 1/9, w_{a=\{5..8\}} = 1/36$ and c is the propagation speed on the lattice, $c = \delta_x/\delta_t$. Under the afore-mentioned assumption of a low Mach number, and further taking $\{Kn[7], \delta_t, \delta_x\} \to 0$, this model recovers the incompressible Navier-Stokes equations:

$$\nabla \cdot \vec{u} = 0 \,, \tag{9.56}$$

$$\rho \partial_t \vec{u} + \rho \vec{u} \cdot \nabla \vec{u} = -\nabla P + \rho \nu \nabla^2 \vec{u} \tag{9.57}$$

with an isothermal equation of state:

$$P = c_s^2 \rho \,, \tag{9.58}$$

where P is the pressure. The viscosity of the fluid is related to the relaxation parameter τ by the equation

$$\nu = c_s^2 (\tau - 1/2) \frac{\delta_x^2}{\delta_t} \Rightarrow \tau = \frac{\nu}{c_s^2}\frac{\delta_t}{\delta_x^2} + \frac{1}{2} \xrightarrow{c_s^2|_{D2Q9}=1/3} \tau_{D2Q9} = 3\nu\frac{\delta_t}{\delta_x^2} + \frac{1}{2} \tag{9.59}$$

The proof of these results follows from the Chapman-Enskog analysis. Eq. (9.59) provides a straightforward method for adjusting the fluid viscosity in the model. It is obvious that $\tau \geq 0.5$ is required in order to ensure a positive viscosity. The limit $\tau \to 0.5$ corresponds to the inviscid flow, while the $\tau \to \infty$ limit represents the Stokes (creeping) flow. The model described so far is only applicable to athermal liquids. While there are many flow situations which can be attributed to this class, thermal effects are often essential to many natural phenomena. A suitable approach consists of solving the passive scalar equation for temperature on a separate lattice. The temperature field is

[7] The assumption of $Kn \equiv \frac{\lambda}{L} \to 0$ is a requirement for continuum models to apply, hence it is not specific to LBM.

influenced by the fluid advection, and influences the fluid through a buoyancy term. This approach is only valid in the Boussinesq approximation, which is a reasonable assumption for many flows (for example, in ocean flows). The LB evolution algorithm is the same on the temperature lattice, but with different equilibrium DFs. Also, because the macroscopic quantity is a scalar (in contrast to the LBM for the velocity field, which is a vector), a lattice with fewer velocity directions is sufficient (D2Q5). The evolution equation on the temperature lattice is described by the same type of LB equation:

$$\underbrace{g_a(\vec{x}+\vec{e}_a\delta_t, t+\delta_t) = g_a(\vec{x},t)}_{\text{Streaming}} - \underbrace{\frac{[g_a(\vec{x},t) - g_a^{eq}(\vec{x},t)]}{\tau_T}}_{\text{Collision}}, \tag{9.60}$$

The macroscopic temperature is recovered by summation:

$$T = \sum_{i=0}^{4} g_i \tag{9.61}$$

The main difference however lies in modified equilibrium distributions:

$$g_i^{eq} = T w_{T,i} \left[1 + 3\vec{e_{T,i}} \cdot \vec{u}\right] \tag{9.62}$$

where the weights on the thermal lattice read $w_{i=0} = 1/3, w_{i=\{1..4\}} = 1/6$, and the thermal diffusivity is related to the thermal relaxation time τ_T through:

$$\tau_T = 3\kappa\frac{\delta_t}{\delta_x^2} + 1/2 \tag{9.63}$$

The back-coupling to the velocity field is accomplished through an additional force term in the RHS Eq. (9.54):

$$dF_i = -3w_i\rho\beta g(T - T_0)(\vec{e}_i \cdot \hat{j}) \tag{9.64}$$

9.4.2 Simulation set-up of the Rayleigh-Bénard convection

An important part of any numerical simulation is relating the simulation input parameters and output results to the exact flow we intend to model. The key concept during these procedures is *dynamic similarity*, which tells us that two flows with different physical parameters are effectively equivalent as long as several dimensionless numbers are the same. This idea is of special importance in experimental and numerical fluid dynamics (e.g., sections 1.4, 7.5). Similarily, in CFD, the fluid solver usually works in a different lengthscale than the original, physical system that is to be simulated. We can distinguish **3** different frames of reference in a simulation, described below. The dimensionless system may seem like an unnecessary complication in the beginning, but it reflects the fact that flows are often given in the literature in this form.

1. **Physical system:** is the actual system that we intend to simulate. Here, we measure things in the usual meters, seconds and kilograms. A problem with this system is that it is very dependent on the units, which are not important to the mathematics behind the PDEs governing the flow. However, any practical application of fluid mechanics has to start from this system and return to it when results are to be reported.
2. **Dimensionless system:** by choosing typical length- and time-scales for our flows, we can non-dimensionalize the equations, which then become more amenable to numerical simulation. Note that, sometimes, it is necessary to choose also a typical mass and/or temperature, depending on the form we take for the macroscopic equations.
3. **Discrete system:** is the coordinate system in which our numerical simulation lives. The input parameters for our simulation propagate from the physical system, through the non-dimensional system until here. Due to reasons of numerical stability, several restrictions are in place at this level, as will be discussed during the practical examples below.

The application we are looking at is the two-dimensional convection driven by a temperature gradient (Rayleigh-Bénard convection). The geometry consists of a rectangular channel, with periodic BCs at the sides and no-slip and constant temperature BCs on the top and bottom walls (section 2.2). Now we can non-dimensionalize the equations by choosing some typical values

for lengthscale $\boldsymbol{L}$ and timescale $\boldsymbol{T}$ of the system. As a reference length $\boldsymbol{L}$, we take the distance between the two walls. We also need a value for scaling our temperature. Since we are imposing a specific temperature difference throughout our fluid domain, the temperature values will be within this range everywhere, and it makes sense to scale temperature by this value $(\boldsymbol{\Delta T})$. The presence of the gravitational constant in the equations provides us a natural timeframe. The first guess would be to take $\boldsymbol{g = L/T^2}$, but we can make a better choice which also allows us to cancel-out the thermal expansion coefficient in the dimensionless system, namely:

$$\boldsymbol{g = \frac{L}{\alpha(\Delta T)T^2} \Rightarrow T = \sqrt{\frac{L}{g\alpha(\Delta T)}}} \tag{9.65}$$

The physical quantities can then be written in terms of the dimensionless ones as $\boldsymbol{p = \rho_0 \frac{L^2}{T^2} p_d}$ and for temperature $\boldsymbol{T = T_d(\Delta T) + T_0}$. Plugging-in these expressions into the eqs. in section 2.2 we eventually obtain:

$$\boldsymbol{\nabla_d \cdot \vec{u_d} = 0} \tag{9.66}$$

$$\boldsymbol{\partial_{t_d} \vec{u_d} + (\vec{u_d} \cdot \nabla_d)\vec{u_d} = -\nabla_d p_d + \sqrt{\frac{Pr}{Ra}} \nabla_d^2 \vec{u_d} + T_d \hat{j}} \tag{9.67}$$

$$\boldsymbol{\partial_{t_d} T_d + \nabla_d \cdot (\vec{u_d} T_d) = \sqrt{\frac{1}{RaPr}} \nabla_d^2 T_d} \tag{9.68}$$

Where $\boldsymbol{Ra}$ and $\boldsymbol{Pr}$ are the characteristic Rayleigh and Prandtl numbers of the system, defined as

$$\boldsymbol{Pr} \equiv \frac{\nu}{\kappa} \tag{9.69}$$

$$\boldsymbol{Ra} \equiv \frac{g\alpha(\Delta T)L^3}{\nu\kappa} = Pr \cdot \frac{g\alpha(\Delta T)L^3}{\nu^2} \tag{9.70}$$

$$\xrightarrow{eq.9.65} \boldsymbol{\nu} = \frac{T}{L^2}\nu = \sqrt{\frac{Pr}{Ra}}; \quad \kappa = \sqrt{\frac{1}{RaPr}} \tag{9.71}$$

The temperature BCs become in the dimensionless system:

$$\boldsymbol{T_{d,hot}} = \mathbf{1}$$
$$\boldsymbol{T_{d,cold}} = \mathbf{0}$$

Discretization of the dimensionless system Let us denote by $\boldsymbol{N}$ the number of gridpoints we use to discretize and by $\boldsymbol{N_{iter}}$ the number of time iterations which will resolve our unit timescale $\boldsymbol{T_d}$. We then have the following discrete space- and time-step in the dimensionless system:

$$\boldsymbol{\delta_x} = \frac{\mathbf{1}}{\boldsymbol{N} - \mathbf{2}}; \quad \boldsymbol{\delta_t} = \frac{\mathbf{1}}{\boldsymbol{N_{iter}} - \mathbf{1}} \tag{9.72}$$

Note that for computing the space-step we need to subtract $\mathbf{1}$ *because* $\boldsymbol{p}$ *points always delimitate* $\boldsymbol{p} - \mathbf{1}$ *segments, and* $(\mathbf{2} \times \mathbf{0.5}) = \mathbf{1}$ *due to the interpretation of the horizontal walls half-way between* $\mathbf{1}^{\boldsymbol{st}}$ *and* $\mathbf{2}^{\boldsymbol{nd}}$ *(respectively half-way between* $\boldsymbol{N} - \mathbf{1}^{\boldsymbol{th}}$ *and* $\boldsymbol{N}^{\boldsymbol{th}}$*) lattice rows. For time-steps, we obviously do not have the second issue, thus we only subtract* $\mathbf{1}$*.*

In a sense, we repeat the procedure we applied to non-dimensionalize the original equations, except that we use $\boldsymbol{\delta_x}$ and $\boldsymbol{\delta_t}$ instead of the previous $\boldsymbol{L}$ and $\boldsymbol{T}$. There is no need to rewrite the equations, since we are interested at this stage only on the parameters that we need to provide to our simulation to get the desired flow. We can easily write expressions for the most relevant quantities in the discrete (LB) system:

$$\vec{\boldsymbol{u_{lb}}} = \frac{\boldsymbol{\delta_t}}{\boldsymbol{\delta_x}}\vec{\boldsymbol{u_d}}; \quad \boldsymbol{g_{lb}} = \frac{\boldsymbol{\delta_t^2}}{\boldsymbol{\delta_x}}\boldsymbol{g_d};$$
$$\boldsymbol{\nu_{lb}} = \frac{\boldsymbol{\delta_t}}{\boldsymbol{\delta_x^2}}\boldsymbol{\nu_d} = \frac{\boldsymbol{\delta_t}}{\boldsymbol{\delta_x^2}}\sqrt{\frac{\boldsymbol{Pr}}{\boldsymbol{Ra}}}; \quad \boldsymbol{\kappa_{lb}} = \frac{\boldsymbol{\delta_t}}{\boldsymbol{\delta_x^2}}\boldsymbol{\kappa_d} = \frac{\boldsymbol{\delta_t}}{\boldsymbol{\delta_x^2}}\sqrt{\frac{\mathbf{1}}{\boldsymbol{RaPr}}}; \tag{9.73}$$

In order to ensure that the compressibility effects do not become significant, a general rule is to keep $\boldsymbol{\delta_t} \sim \boldsymbol{\delta_x^2}$. Let us denote by $\boldsymbol{\beta}$ the proportionality factor (i.e. $\boldsymbol{\delta_t} = \boldsymbol{\beta}\boldsymbol{\delta_x^2}$). The choice of $\boldsymbol{\beta}$ is not very obvious. If it is chosen too big, the timesteps get too large and the accuracy of the simulation decreases. However, if $\boldsymbol{\beta}$ is too small, the simulation takes a long time. This means

a compromise for β has to be found (Here, we choose $\beta = 11.18$ for $\delta_x = 0.02$). Once the number of gridpoints is given, this relation gives number of timesteps to resolve t_{0p}.
We also need to choose a representative value for the temperature, but we can simply pick a one-to-one mapping from the dimensionless system.

$$T_{lb} = T_d \tag{9.74}$$

We could write the formulae for converting the results back to the dimensionless and/or physical system.

9.4.3 System preparations and running a simulation

There are only a few parameters that define the behavior of the system: The number of gridpoints (*lx*, *ly*) defines the size of the lattice and thereby directly affects the accuracy of the results. On the one hand we get better results with a finer grid but on the other hand the computational cost increases dramatically. The parameter *N_t0* descibes the maximal simulation time in units of t_{0d}. For a given physical system t_{0d} can be calculated using eq. 9.65. *N_t0* should be high enough to overcome the inital conditions.

Remember that the Rayleigh (*Ra*) and Prandtl (*Pr*) numbers are dimensionless numbers that define the character of the flow. *Pr* is the ratio of the viscosity ν and the thermal conductivity k. *Ra* describes the heat transfer of a buoyancy driven flow. Some results for different sets of parameters can be seen in figure 9.4. As seen in section 9.4.2 *beta* is the factor that couples the spatial and temporal step sizes of the lattice. As for the grid resolution, a compromise between accuracy of the results and computing time has to be found!

Run simulation After installation run R and change the working directory of R to the path where the *.r-files of the model are located:

```
setwd('Path/of/Rayleigh_Benard_model')
```

If all parameters are set properly, the model is loaded and executed by the command

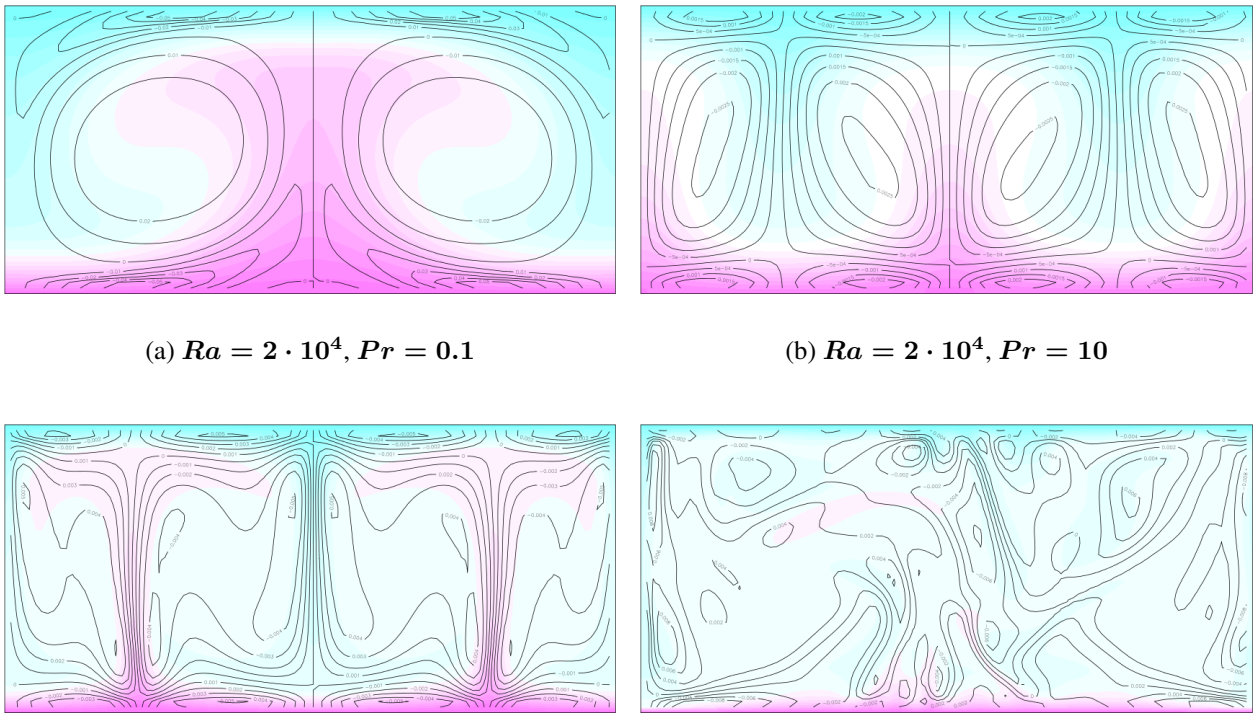

(a) $\boldsymbol{Ra = 2 \cdot 10^4}$, $\boldsymbol{Pr = 0.1}$

(b) $\boldsymbol{Ra = 2 \cdot 10^4}$, $\boldsymbol{Pr = 10}$

(c) $\boldsymbol{Ra = 5 \cdot 10^5}$, $\boldsymbol{Pr = 10}$

(d) $\boldsymbol{Ra = 1 \cdot 10^7}$, $\boldsymbol{Pr = 10}$

Figure 9.4: Four examples of the flow for different sets of $\boldsymbol{Ra}$ and $\boldsymbol{Pr}$. The contours show lines of constant vorticity; the colors in the background display the temperatures (purple - warm, blue - cold).

```
source('rayleigh-benard.R')
```

After the simulation has completed the results can be found in the folder defined by the parameter *out_dir*. For a new run, the old directory has to be removed or renamed. All necessary files and parameters are shortly described here. Your application should come with the following files:

- rayleigh-benard.R | The R source code
- rb_functions.R | Some extra R functions needed by the model
- rb_plot_functions.R | Some R functions for plotting the results

There are two different types of parameters that can be edited: the 'model parameters' (which define the 'physical' values needed for the simulation), and the 'output parameters' (which define the frequency and kind of output).

Here is some R-code of the code calculating the macroscopic moments rho, ux, uy, T:

```
#Compute macroscopic values
  rho = colSums(flIn, dims=1);
  T = colSums(TIn, dims=1);
  ux = colSums( cx_fl*flIn, dims=1 ) / rho;
  uy = colSums( cy_fl*flIn, dims=1 ) / rho;
```

which is related to (9.52, 9.53) and (9.61), respectively. *cx_fl* and *cy_fl* denote the 9-dimensional momentum component ($\vec{e}_a$ in 9.53) and are related to the microscopic velocities $\vec{e}$ in the distribution function $f(\vec{x}, \vec{e}, t)$ of the Boltzmann dynamics (9.26). The main part of the code is the collision step for momentum and temperature:

```
#Collision Step
  #Fluid momentum
  for (i in idxRangeFluid){
    cu_fl = 3* (cx_fl[i] * ux + cy_fl[i] * uy);
    flEq= rho * w_fl[i] *
        (1 + cu_fl + 0.5 * cu_fl^2 - 1.5 * (ux^2 + uy^2));
    force = 3* w_fl[i]* rho * (T-T0)*
        (cx_fl[i] * g[1] + cy_fl[i] * g[2])/(T_bot - T_top);
    flOut[i,,] = (1.-omega_fl)*flIn[i,,] + omega_fl*flEq + force;
  }

  #Temperature
  for (i in idxRangeTemp){
    cu_T = 3* (cx_T[i] * ux + cy_T[i] * uy);
    TEq = T * w_T[i] * (1 + cu_T);
    TOut[i,,] = (1.-omega_T)*TIn[i,,] + omega_T*TEq;
  }
```

where *fl_Eq* and *T_Eq* denote the local Maxwell-Boltzmann single-particle distribution function.

Exercise 66 – Investigations with the LB-model

1. Vary the Rayleigh and the Prandtl number by $\boldsymbol{R_a} = \mathbf{20000, 40000, 60000}$ and $\boldsymbol{Pr} = \mathbf{0.5, 1, 1.5, 5, 10}$ and describe the dynamics (words, figures) ! For high values of $\boldsymbol{R_a}$ the spatial resolution might be chosen higher (to the double). Here are the standart values:

```
lx  = 100;    #Number of horizontal cells
ly  = 52;   #Number of vertical cells
```

2. Vary the initial perturbation and obtain the reversed circulation! Look at the line

```
#Set small trigger to break symmetry
T[lx/2+1, 1] = 1.1 * T_bot;
```

Here, some remarks related to the boundary conditions are in order. When using a Dirichlet boundary condition, one prescribes the value of a variable at the boundary, e.g. temperature or density in our case. When using a Neumann boundary condition, one prescribes the gradient normal to the boundary of a variable at the boundary, e.g. the heat flux or density flux. When using a mixed boundary condition, different types of boundary conditions can be used for different variables (e.g. for temperature and salinity).

In viscous flows, no-slip condition enforced at walls:

-Tangential fluid velocity equal to wall velocity.

-Normal velocity component is set to be zero.

This is realized through a bounce back condition: a particle travelling in the $\boldsymbol{e_1}-$direction is bounced back into the opposite $\boldsymbol{e_5}-$direction. A modified version of the previous problem is an ocean box with solid walls and free slip at the surface (no friction). This is implemented by mirroring (relative to horizontal-axis) the distribution functions in the fluid-lattice:

```
#"Bounce Back" Boundary Conditions for Fluid
  for (i in idxRangeFluid){
    flOut[i,,1] = flIn[opp_fl[i],,1];
    flOut[i,,ly] = flIn[opp_fl[i],,ly];
  }
```

Used when physical geometry of interest and expected flow pattern and the thermal solution are

of a periodically repeating nature (as in the Rayleigh-Bénard problem). This reduces computational effort in problem.

Exercise 67 – Ocean-like circulation

1. Evaluate the effect of different external temperatures (hemispheric, double hemispheric). The R code is

   `ocean_rb.R`

   Here are two options:

```
# Pre-compute imposed temperature-profile on top (linear)
tempTop = array(0, c(lx));
for (x in 2:lx-1) {
  tempTop[x] = THot - (THot-TCold)*(x-2)/(lx-3);
 }
```

   for a single hemisphere, and for a double hemisphere version:

```
# Pre-compute imposed temperature-profile on top (linear+sinus)
tempTop = array(0, c(lx));
bett= 0.2 # right boundary
alph= (0.1-bett)/lx ;
gamma =1.-alph * lx/2 -bett;
for (x in 2:lx-1) {
  tempTop[x] = alph *x + bett + gamma * sin( 3.1416* x/lx);
}
```

   Describe the dynamics with respect to the temperature at the top layer tempTop !

2. In lattice Boltzmann models, it is relatively easy to insert obstacles. The R code is

   `ocean_rb_ridge.R`

   Discuss the influnce of the ridge on the ocean circulation!

3. Manage to change the Rayleigh-Bénard convection from a no-slip to free slip bounday conditions at the top. The upper plate is just removed and we have an air-water interface. What are the differences? Make a plot!

4. Provide a model for the atmospheric cells (the atmosphere is mainly heated from below).

5. Calculate the ocean heat transport in the model and compare it with the estimate in exercise 46! Use dimensionless parameters!

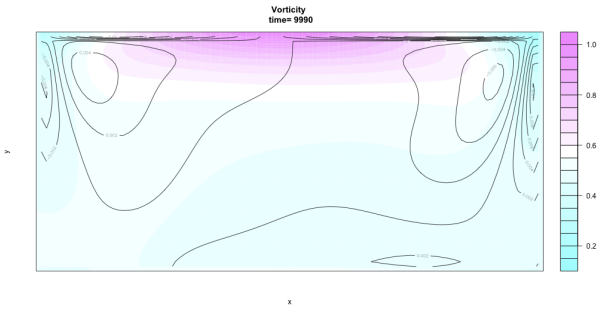

(a) Two hemisphere temperature

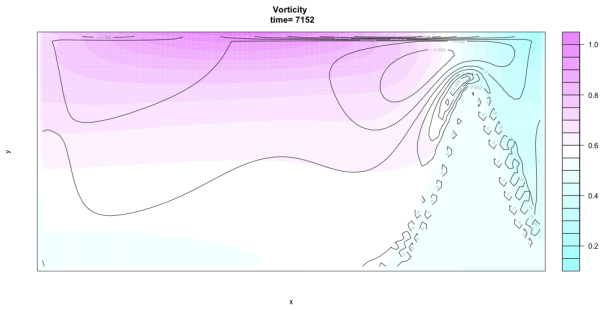

(b) Ridge and a two hemisphere temperature

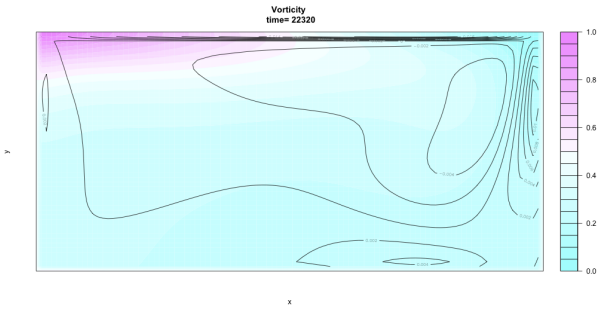

(c) Linear temperature gradient

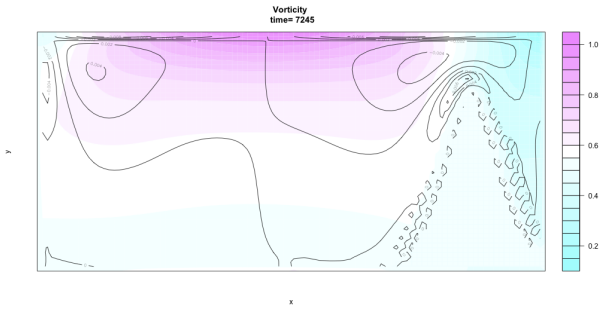

(d) Flow including a ridge

Figure 9.5: Four examples of the ocean flow for different boundary conditions, and fixed Prandtl number=1 and Rayleigh number=45000. The contours show lines of constant vorticity; the colors in the background display the temperatures (purple - warm, blue - cold). For the right scenarios, an obstacle representing an oceanic sill is implemented.

Part IV

Fourth part: Programming and tools

Bibliography

Abramowitz, M. and Stegun, I. A. (1965). Handbook of mathematical functions with formulas, graph, and mathematical tables. *Applied Mathematics Series*, 55:1046.

Arnold, L. (1995). *Random dynamical systems*. Springer.

Arnold, L. (2001). *Hasselmann's program revisited: The analysis of stochasticity in deterministic climate models*, volume 49. Birkhäuser, Boston.

Baker, G. L. and Blackburn, J. A. (2005). *The pendulum: a case study in physics*, volume 8. Oxford University Press Oxford.

Barber, D., Dyke, A., Hillaire-Marcel, C., Jennings, J., Andrews, J., Kerwin, M., Bilodeau, G., McNeely, R., Southon, J., Morehead, M., and Gagnonk, J.-M. (1999). Forcing of the cold event of 8,200 years ago by catastrophic drainage of laurentide lakes. *Nature*, 400(6742):344–348.

Bhatnagar, P., Gross, E. P., and Krook, M. K. (1954). A model for collision process in gases. i. small amplitude processes in charged and neutral one-component system. *Phys. Rev*, 94:511.

Boltzmann, L. (1896). *Vorlesungen über Gastheorie : 2 Volumes (in German)*. Leipzig 1895/98 UB: O 5262-6.

Boltzmann, L. (1995). *Lectures on Gas Theory*. Dover Publ. New York. ISBN 978-0486684550.

Broecker, S. and Peng, T.-H. (1982). *Tracers in the Sea*. Columbia University.

Broecker, W. S. (1987). The biggest chill. *Natural History*, 97(2):74–82.

Broecker, W. S. et al. (1991). The great ocean conveyor. *Oceanography*, 4(2):79–89.

Brüning, R. and Lohmann, G. (1999). Charles s. peirce on creative metaphor: a case study on the conveyor belt metaphor in oceanography. *Foundations of science*, 4(4):389–403.

Bryan, F. (1986). High latitude salinity effects and inter-hemispheric thermohaline circulations. *Nature*, 323(3):301–304.

Buckingham, E. (1914). On physically similar systems; illustrations of the use of dimensional equations. *Physical Review*, 4(4):345–376.

Budyko, M. I. (1969). The effect of solar radiation variations on the climate of earth. *Tellus*, 21:611–619.

Busch, W. (1865). *Max und Moritz (in German); Max and Maurice, a Juvenile History in Seven Tricks* . Braun und Schneider, München.

Cercignani, C. (1987). *The Boltzmann equation and its applications*. Springer New York. ISBN 978-0387966373.

Cercignani, C. (1990). *Mathematical methods in kinetic theory*. Plenum, 2 edition. ISBN 978-0306434600.

Chelton, D. B. and Schlax, M. G. (1996). Global Observations of Oceanic Rossby Waves. *Science*, 272:234–238.

Chen, D., Gerdes, R., and Lohmann, G. (1995). A 1-d atmospheric energy balance model developed for ocean modelling. *Theoretical and Applied Climatology*, 51:25–38.

Chorin, A. J. and Hald, O. H. (2006). Stochastic tools in mathematics and science. surveys and tutorials in the applied mathematical sciences, vol. 1.

Chorin, A. J., Kast, A. P., and Kupferman, R. (1999). Unresolved computation and optimal predictions. *Communications on pure and applied mathematics*, 52(10):1231–1254.

Chorin, A. J., Kupferman, R., and Levy, D. (2000). Optimal prediction for hamiltonian partial differential equations. *Journal of Computational Physics*, 162(1):267–297.

Courant, R., Friedrichs, K., and Lewy, H. (1928). Über die partiellen Differenzengleichungen der mathematischen Physik. *Mathematische Annalen*, 100:32–74.

Courant, R., Friedrichs, K., and Lewy, H. (1967). On the partial difference equations of mathematical physics. *IBM J. Res. Dev.*, 11(2):215–234.

Dansgaard, W., Johnsen, S., Clausen, H., Dahl-Jensen, D., Gundestrup, N., Hammer, C., C.S. Hvidberg, J. S., Sveinbjoernsdottir, A., Jouzel, J., and Bond, G. (1993). Evidence for general instability of past climate from a 250-kyr ice-core record. *Nature*, 364:218–220.

d'Humieres, D., Bouzidi, M., and Lallemand, P. (2001). Thirteen-velocity three-dimensional lattice boltzmann model. *PRE*, 63(6, Part 2).

Dijkstra, H., Raa, L. T., and Weijer, W. (2004). A systematic approach to determine thresholds of the ocean's thermohaline circulation. *Tellus A*, 56 (4):362.

Doedel, E. J., Champneys, A. R., Fairgrieve, T. F., Kuznetsov, Y. A., Sandstede, B., and Wang, X. (1997). Continuation and bifurcation software for ordinary differential equations (with homcont). *Available by anonymous ftp from ftp cs concordia ca, directory pub/doedel/auto*.

Egger, J. (2001). Master equations for climatic parameter sets. *Climate Dynamics*, 18(1-2):169–177.

Einstein, A. (1905). Investigations on the theory of the brownian movement. *Ann. der Physik*, 17:549–560.

Einstein, A. (1926). Die Ursache der Mäanderbildung der Flußläufe und des sogenannten Baerschen Gesetzes. *Naturwissenschaften*, 14:223–224.

Evans, D. J. and Morriss, G. (2008). *Statistical mechanics of nonequilibrium liquids*. Cambridge University Press.

Fairbanks, R. G. (1989). A 17, 000-year glacio-eustatic sea level record: influence of glacial melting rates on the younger dryas event and deep-ocean circulation. *Nature*, 342(6250):637–642.

Feigenbaum, M. J. (1980). The transition to aperiodic behaviour in turbulent systems. *Commun. Math. Phys.*, 77.

Flammer, C. (1957). *Spheroidal wave functions*. Stanford University Press.

Frisch, U. (1996). *Turbulence: the legacy of A.N. Kolmogorov*. Cambridge University Press. ISBN 0-521-45103-5.

Gerkema, T., Zimmerman, J., Maas, L., and Van Haren, H. (2008). Geophysical and astrophysical fluid dynamics beyond the traditional approximation. *Reviews of Geophysics*, 46(2).

Gill, A. E. (1982). *Atmosphere-ocean dynamics*, volume 30. Academic Press. International Geophysics Series.

Givon, D., Kupferman, R., and Stuart, A. (2004). Extracting macroscopic dynamics: model problems and algorithms. *Nonlinearity*, 17(6):R55.

Gottwald, G. (2010). On recent trends in climate dynamics. *AMS Gazette*, 37(5).

Grassberger, P. and Procaccia, I. (1983). Measuring the strangeness of strange attractors. *Physica D: Nonlinear Phenomena*, 9(2):189–208.

Haken, H. (1996). Slaving principle revisited. *Physica D: Nonlinear Phenomena*, 97(1):95–103.

Haney, R. L. (1971). Surface thermal boundary conditions for ocean circulation models. *Journal of Physical Oceanography*, 1:241–248.

Hasselmann, K. (1976). Stochastic climate models. Part I. Theory. *Tellus*, 6:473–485.

He, X. and Luo, L. S. (1997). Theory of the lattice Boltzmann method: From the Boltzmann equation to the lattice Boltzmann equation. *Phys. Rev. E*, 56(6):6811–6817.

Holton, J. R. (2004). *An Introduction to Dynamic Meteorology*. Elsevier Academic Press, Burlington, MA.

Kambe, T. (2007). *Elementary Fluid Mechanics*. World Scientific Publishing.

Kuznetsov, Y. A. (1998). *Elements of applied bifurcation theory*, volume 112. Springer, New York.

Landau, L. D. and Lifshitz, E. M. (1959). *Fluid Mechanics*, volume 6 of *Course of Theoretical Physics*. Pergamon Press, Oxford.

Langevin, P. (1908). On the theory of brownian motion. *Comptes Rendues*, 146:530–533.

Leith, C. (1975). Climate response and fluctuation dissipation. *Journal of the Atmospheric Sciences*, 32(10):2022–2026.

Lohmann, G. (2003). Atmospheric and oceanic freshwater transport during weak atlantic overturning circulation. *Tellus A*, 55(5):438–449.

Longuet-Higgins, M. S. (1968). The eigenfunctions of laplace's tidal equations over a sphere. *Philosophical Transactions for the Royal Society of London. Series A, Mathematical and Physical Sciences*, pages 511–607.

Lorenz, E. (1982). Atmospheric predictability experiments with a large numerical model. *Tellus A*, 34:505–513.

Lorenz, E. N. (1960). Maximum simplification of the dynamic equations. *Tellus*, 12(3):243–254.

Lorenz, E. N. (1963). Deterministic nonperiodic flow. *Journal of the atmospheric sciences*, 20(2):130–141.

Lorenz, E. N. (1976). Nondeterministic theories of climatic change. *Quaternary Research*, 6(4):495–506.

Lorenz, E. N. (1984). Irregularity: a fundamental property of the atmosphere*. *Tellus A*, 36(2):98–110.

Lucarini, V., Blender, R., Herbert, C., Pascale, S., Ragone, F., and Wouters, J. (2014). Mathematical and physical ideas for climate science. *Rev. Gephys.*

Maas, L. R. (1994). A simple model for the three-dimensional, thermally and wind-driven ocean circulation. *Tellus A*, 46(5):671–680.

Manabe, S. and Stouffer, R. (1993). Century-scale effects of increased atmospheric $\boldsymbol{CO_2}$ on the ocean atmosphere system. *Nature*, 364:215–218.

Mandelbrot, B. B. (1967). How long is the coast of britain: Statistical self-similarity and fractal dimension. *Science*, 155:636–638.

Mandelbrot, B. B. (1983). *The fractal geometry of nature*. Macmillan.

Matsuno, T. (1966). Quasi-geostrophic motions in the equatorial area. *J. Meteor. Soc. Japan*, 44(1):25–43.

Mori, H. (1965). Transport, collective motion, and brownian motion. *Progress of Theoretical Physics*, 33(3):423–455.

Mori, H., Fujisaka, H., and Shigematsu, H. (1974). A new expansion of the master equation. *Progress of Theoretical Physics*, 51(1):109–122.

Müller and Maier-Reimer (2000). Trapped rossby waves. *Phys. Rev. E*, 61:1468 – 1485.

Müller, D., Kelly, B., and O'brien, J. (1994). Spheroidal eigenfunctions of the tidal equation. *Physical review letters*, 73(11):1557.

Müller, D. and O'Brien, J. (1995). Shallow water waves on the rotating sphere. *Physical Review E*, 51(5):4418.

Olbers, D. (2001). A gallery of simple models from climate physics. *In: Stochastic Climate Models, Progress in Probability (Eds.: P. Imkeller and J. von Storch)*, 49:3–63.

Peitgen, H.-O. and Richter, P. (1986). *The Beauty of Fractals*. Heidelberg: Springer-Verlag.

Proudman, J. (1916). On the motion of solids in a liquid possessing vorticity. *Proc. R. Soc. Lond. A*, 92:408–424.

Rahmstorf, S. (1996). On the freshwater forcing and transport of the Atlantic thermohaline circulation. *Climate Dynamics*, 12:799–811.

Rayleigh, L. (1916). On convection currents in a horizontal layber of fluid, when the higher temperature is on the under side. *Phil. Mag.*, 6:529–546.

Rooth, C. (1982). Hydrology and ocean circulation. *Progress in Oceanography*, 11:131–149.

Rossby, C.-G. (1939). "relation between variations in the intensity of the zonal circulation of the atmosphere and the displacements of the semi-permanent centers of action". *Journal of Marine Research*, 2 (1):38–55.

Saltzman, B. (1962). Finite amplitude free convection as an initial value problem – i. *Journal of the Atmoshpheric Sciences*, 19:329–341.

Shannon, C. E. (1948). A Mathematical Theory of Communication. *Bell System Technical Journal*, 27 (3):379–423.

Stommel, H. (1961). Thermohaline convection with two stable regimes of flow. *Tellus*, 13:224–230.

Strogatz, S. (2000). *Non-linear Dynamics and Chaos: With applications to Physics, Biology, Chemistry and Engineering*. Perseus Books.

Taylor, G. (1917). Motion of solids in fluids when the flow is not irrotational. *Proc. R. Soc. Lond. A*, 93:92–113.

Townsend, S., Lenosky, T., Muller, D., Nichols, C., and Elser, V. (1992). Negatively curved graphitic sheet model of amorphous carbon. *Physical Review Letters*, 69(6):921–924.

Tritton, D. J. (1988). *Physical Fluid Dynamics*. Oxford University Press, Science Publication. ISBN 978-0-19-854493-7.

Uhlenbeck, G. E. and Ornstein, L. S. (1930). On the theory of the brownian motion. *Physical review*, 36(5):823.

van Kampen, N. G. (1981). *Stochastic processes in physics and chemistry*. North Holland. IISBN 978-0-444-52965-7.

Wüst, G. (1935). Schichtung und Zirkulation des Atlantischen Ozeans. Das Bodenwasser und die Stratosphäre. *Wiss. Ergebn. Dtsch. Atlant. Exped. 'Meteor' 1925-1927*, 6(1):1–288.

Zwanzig, R. (1960). Ensemble method in the theory of irreversibility. *The Journal of Chemical Physics*, 33:1338.

Zwanzig, R. (1980). Problems in nonlinear transport theory. In *Systems far from equilibrium*, pages 198–225. Springer.

Zwanzig, R. (2001). *Nonequilibrium statistical mechanics*. Oxford University Press, USA.